Estuaries and Coasts (2023) 46:2023–2044
https://doi.org/10.1007/s12237-022-01137-y

SPECIAL ISSUE: LOW INFLOW ESTUARIES

Variability in Phytoplankton Biomass and Community Composition in Corpus Christi Bay, Texas

Sarah A. Tominack[1] · **Michael S. Wetz**[1]

Received: 1 June 2022 / Revised: 8 October 2022 / Accepted: 9 October 2022 / Published online: 14 November 2022

Abstract

Corpus Christi Bay is a shallow, wind-driven lagoon located on the semi-arid South Texas coast that has a rapidly urbanizing watershed. Projections indicate that this region will become warmer and drier and will support an increasing urban population over the next several decades. Here, a 27-month field study was undertaken to quantify phytoplankton biovolume, community composition, and relationships with environmental drivers. Phytoplankton biovolume varied unimodally with a peak in biovolume from spring through summer followed by a decline into fall and winter. Phytoplankton growth was related to nutrient availability during the spring and summer, while water temperature and factors affecting flushing were important during the fall and winter. Regions with more restricted circulation patterns (i.e., man-made canals) were found to support higher standing crops of phytoplankton and the occurrence of high biovolume blooms. Diatoms were dominant during the winter and spring, dinoflagellates were dominant during the summer and fall, and picophytoplankton groups were important during spring, summer, and fall. These results suggest that nutrient and physical conditions interact to determine phytoplankton biomass and community composition and contribute to our ability to project potential impacts of future increases in human populations in the watershed, decreasing precipitation due to climate change, and increasing frequency of short-lived flood events.

Keywords Estuary · Low inflow · Phytoplankton · Texas

Introduction

Estuaries are highly dynamic systems at the confluence of rivers and the ocean and are subject to environmental fluctuations acting on multiple time scales (Cloern and Jassby 2010; Paerl et al. 2010; Zingone et al. 2010). Phytoplankton is at the base of marine food webs and are important primary producers in many estuaries (Cloern and Dufford 2005; Paerl et al. 2010; Cloern et al. 2014). Variability in freshwater inflows is a particularly important factor influencing estuarine phytoplankton dynamics due to the role they play in driving external nutrient loading, residence time, and light conditions (Paerl et al. 2010; Peierls et al. 2012; Roelke et al. 2013; Dorado et al. 2015). For example, in river-dominated estuaries, nutrient loading often scales to the level of freshwater inflows and consequently so does phytoplankton growth and primary production up to a certain inflow level, after which flushing and/or light conditions can become limiting (Mallin et al. 1993; Wetz et al. 2011). This is not always the case in lagoonal estuaries however, where ample stores of internally cycled nutrients can support phytoplankton growth even when inflows are low (McCarthy and Bronk 2008; Glibert et al. 2010; Reyna et al. 2017; Geyer et al. 2018; Cira et al. 2021). Freshwater inflow variability can also have a major influence on phytoplankton community composition (Paerl et al. 2010; Peierls et al. 2012; Roelke et al. 2013; Dorado et al. 2015). In high flow conditions with high nutrient concentrations and short residence time, taxa with relatively fast growth rates (i.e., diatoms, cryptophytes, and chlorophytes) are more likely to be favored. In contrast, during low flow conditions with low nutrient concentrations and longer residence time, slower growing taxa (i.e., dinoflagellates) often dominate (Cloern and Dufford 2005; Paerl et al. 2010). Seasonal changes in water temperature, light, and nutrient availability are often

Communicated by James L. Pinckney

✉ Michael S. Wetz
michael.wetz@tamucc.edu

[1] Harte Research Institute for Gulf of Mexico Studies, Texas A&M University – Corpus Christi, Corpus Christi, TX, USA

important drivers of phytoplankton biomass, with the greatest proportion of high biomass events recorded during the spring and the lowest during the winter on a global scale (Cloern and Jassby 2008, 2010). Additionally, the ecophysiology of different phytoplankton groups often results in predictable patterns of seasonal community succession, with diatoms tending to dominate in cooler and/or wetter seasons and dinoflagellates tending to dominate during warmer and/or drier seasons (Cloern 1999; Örnólfsdóttir et al. 2004; Cloern and Jassby 2008, 2010).

Watershed land use at the local and regional scale represents a factor influencing nutrient delivery, and ultimately phytoplankton populations, in coastal environments. Increases in urban and suburban development have been shown to increase nutrient loads and change the ratio of various nutrients delivered to estuaries (Paerl et al. 2014; Jordan et al. 2018). In Florida's Indian River Lagoon for example, portions of the estuary with greater anthropogenic influence on watershed land use demonstrated higher mean phytoplankton biovolume than regions with more pristine watersheds (Phlips et al. 2011). Wastewater treatment plant (WWTP) effluent and stormwater runoff tend to deliver high nitrogen and phosphorus loads to receiving waterbodies (Gilabert 2001; Dillon and Chanton 2005; Glibert and Burkholder 2011; Davidson et al. 2014), but often deliver less dissolved silicate than riverine sources of freshwater, potentially leading to the selection of non-diatom taxa over diatoms and/or increased prevalence of harmful algal bloom (HAB) forming diatoms with lower silica requirements (i.e., *Pseudo-nitzschia* spp.) (Roelke et al. 1997; Quigg et al. 2013; Parsons and Dortch 2002; Davidson et al. 2014).

Evidence is emerging that low-inflow lagoonal estuaries may be particularly susceptible to anthropogenic nutrient inputs (Ferreira et al. 2005; Bricker et al. 2008). For example, several studies have shown the potential for very high biomass blooms in these types of estuaries, including harmful taxa that are suited to low rates of flushing (i.e., dinoflagellates and pelagophytes) commonly found in these types of systems (Hemraj et al. 2017; Cira et al. 2021; Glibert et al. 2021; Lemley et al. 2017, 2021). Despite this, there is a paucity of data on phytoplankton dynamics and anthropogenic influences on phytoplankton communities from low-inflow estuaries. Here, a 27-month field study was conducted in Corpus Christi Bay (CCB), Texas, across six sites representing different levels of anthropogenic influence. CCB has a neutral freshwater inflow balance and salinity levels that are typical of ocean conditions (Montagna et al. 2009), although in recent decades hypersalinty has been observed during drought due to both the lack of rainfall and a long-term decrease in inflows due to damming (Bugica et al. 2020). To date, there have been no comprehensive studies on phytoplankton dynamics in this ecologically and economically important estuary. Studies addressing the spatial-temporal distribution of phytoplankton and potential environmental drivers are necessary to establish an understanding of contemporary dynamics and to provide context for projections of future change in response to increased human population growth, land use change, increased frequency of droughts, and continued declines in freshwater inflows. This study focused on the western and southern shorelines of CCB to assess the role of anthropogenic activities (urbanization), structural modifications to the estuarine environment (canal construction), and freshwater inflows (riverine and stormwater drainage) in driving phytoplankton dynamics in a low-inflow estuary, CCB.

It was hypothesized that both phytoplankton biovolume and community composition would display spatial variability in response to different levels of anthropogenic influence on nutrient availability. Specifically, regions of greatest anthropogenic nutrient influence would display higher nutrient concentrations (Paerl et al. 2014; Jordan et al. 2018) and support the highest overall phytoplankton biovolume (Flint 1984; Phlips et al. 2011). Additionally, it was hypothesized that a greater proportion of community biovolume would be attributed to dinoflagellate and cryptophyte taxa in the anthropogenically influenced regions due to the competitive ability of those taxa to high nutrient loads and altered (from natural conditions) nutrient forms (findings from Cloern and Dufford (2005), Burkholder et al. (2008), and Davidson et al. (2014)). Seasonal fluctuations in temperature, rainfall, and wind were also hypothesized to be important factors influencing phytoplankton biovolume, with maxima expected in summer months due to higher temperatures, lower frequency of washout events, and lower wind speeds (Flint 1984; Pennock et al. 1999). These factors, along with nutrient availability, were hypothesized to play a role in seasonal variation in phytoplankton community structure, with diatoms expected to be important in cooler months, and the relative contributions of flagellated taxa increasing in the fall with increased water column stability (Holland et al. 1975). In addition to representing the first study of its kind in a local estuary (Corpus Christi Bay-Upper Laguna Madre), this study is novel because there are few studies on nutrient-phytoplankton dynamics in similar low-inflow estuaries worldwide despite the numerical importance of these types of estuaries (Largier and Behrens 2010).

Methods

Study Area

CCB is a shallow (~3 m, ship channel ~15 m), microtidal (~0.3 m range), wind-driven system (~18 km h^{-1} yearly mean; Ritter and Montagna 1999; Islam et al. 2014; Turner et al. 2015) that comprises the largest portion of the Nueces

Estuary. CCB is located on the semi-arid South Texas coast and is separated from the Gulf of Mexico by Padre Island, with two inlets for water exchange (Packery Channel and Aransas Pass). Inflow from the Nueces River has declined since the construction of dams in 1958 and 1982 (Montagna et al. 2009; Fig. 1). The neutral inflow balance that is now present leads to a relatively long residence time (> 5 months–1 year) and a generally well-mixed water column. CCB is also susceptible seasonal hypoxia (Ritter and Montagna 1999) and *Karenia brevis* red tides, with the latter showing a marked increase in frequency of occurrence since the mid-1990s (Tominack et al. 2020).

The lower reaches of the CCB watershed are heavily urbanized, with the city of Corpus Christi (pop. 317,863) lying adjacent to the bay. Corpus Christi has undergone rapid population growth over the past 2 decades (8.5% increase 2000 to 2010; 7% increase 2010 to 2019) (U.S. Census Bureau), with an ~13% increase in developed areas occurring from 2001 to 2016, leading to increased stormwater inputs. Stormwater runoff has been shown to increase nutrient concentrations, leading to increased phytoplankton biomass following inputs (Turner et al. 2015). WWTPs are also an influential source of inorganic nutrients, especially in low-inflow systems like CCB (Yeager et al. 2006; Wetz et al. 2017; https://sparrow.wim.usgs.gov/sparrow-southwest-2012/). Bugica et al. (2020) found a "hot spot" of eutrophication in Oso Bay, a sub-bay of CCB, where WWTP effluent has been shown to be a driver of decreasing water quality (Wetz et al. 2016). Another factor negatively impacting the CCB system is the long-term decrease in freshwater inflows due to dam construction and water management (Montagna et al. 2009). Dam construction reduced freshwater inflows by approximately 48% (Montagna et al. 2009) and has been shown to be associated with increases in salinity (Montagna et al. 2009), and decreased loading of riverine N (Dunn 1996) to CCB.

Sampling Sites

Six sampling sites were selected to represent an estuarine nutrient-salinity gradient (Fig. 2). All sampling sites were located along the shoreline to both ensure sampling events could proceed under inclement weather conditions and to assess the direct impacts of anthropogenic stressors (i.e., WWTP effluent and stormwater runoff). Although some observed phytoplankton-nutrient dynamics in these shoreline regions of CCB may not be relevant to dynamics in central CCB, the inclusion of relatively enriched sites (Canal and Oso Inlet) and those that receive point-source and overland runoff (Cole Park and South Shore) allowed for the assessment of "hot spots" of anthropogenic influence where critical habitats (seagrass beds, habitat and foraging grounds for migratory, and resident birds) and humans are in close proximity. In order from lowest level of anthropogenic influence to highest level of anthropogenic influence, site descriptions are as follows. The Laguna Madre site was located in the Upper Laguna Madre, where there is little connectivity with freshwater sources, freshwater inputs are primarily from overland runoff, and human populations are very sparse. The Packery Channel is a man-made inlet between the Gulf of Mexico and the lower CCB and is likely the most well-flushed site in this study. The South Shore site was located along the southern shoreline of CCB and was adjacent to a stormwater runoff drain (~90 m away) that receives inputs from ~5 km^2 of densely populated urban area. Oso Inlet was at the confluence of Oso Bay and CCB, with freshwater sources including Oso Creek and a nearby WWTP effluent pipe. Previous work has shown that the Oso

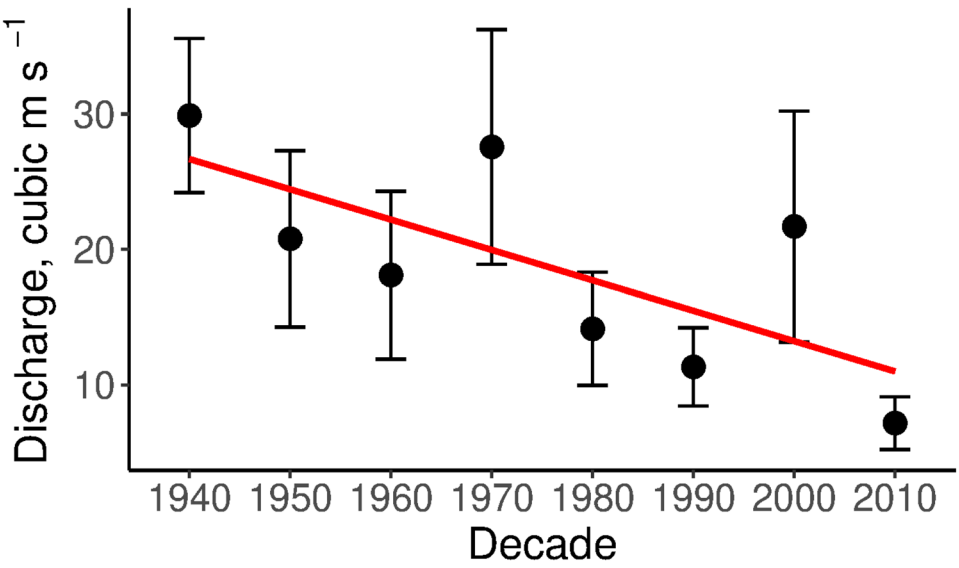

Fig. 1 Mean decadal inflows to the Corpus Christi Bay system from the Nueces River with a regression line demonstrating a decreasing trend between 1940 and 2019. The US Geological Survey stream gauge used for creation of this graph was 8211000. Figure 1 was created using the R statistical software package

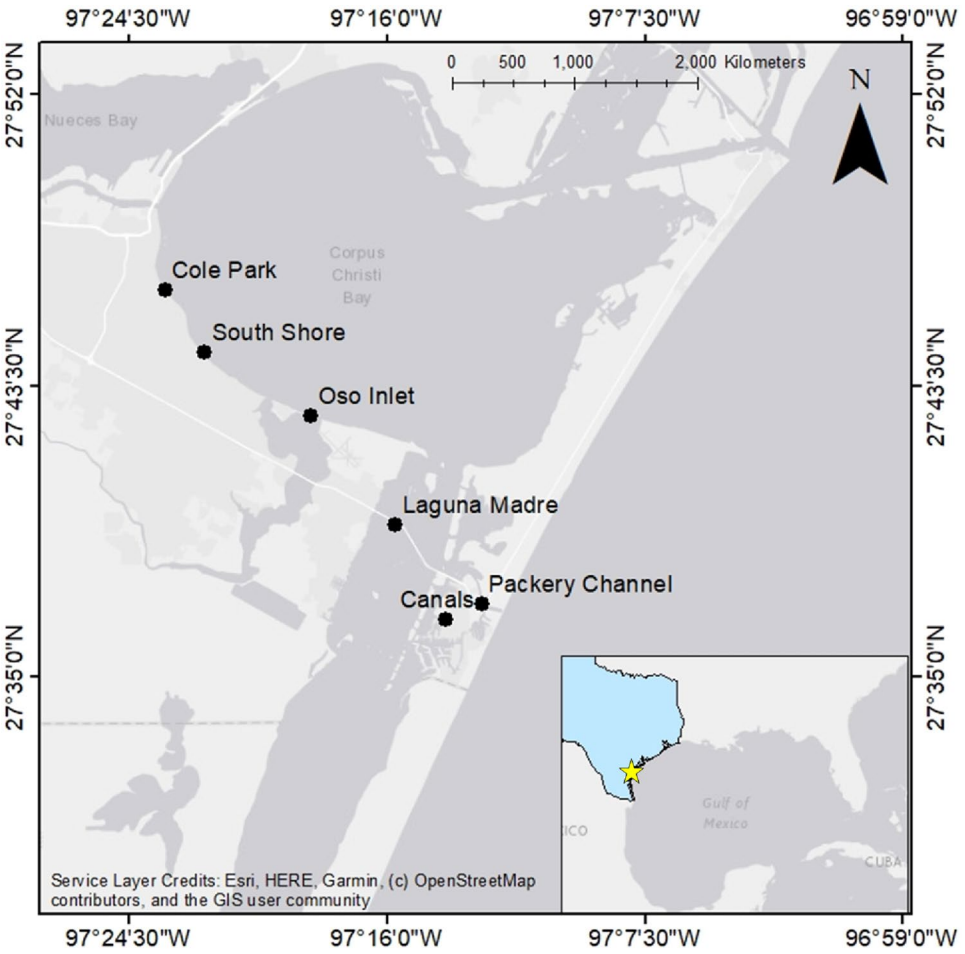

Fig. 2 Location of sampling sites throughout Corpus Christi Bay. Corpus Christi is denoted with a star in the inset map. Figure 2 was created using ArcMap and MSOffice

Bay is heavily impacted by WWTP effluent, as indicated by consistently high nutrient concentration and phytoplankton biomass (Wetz et al. 2016; Wang et al. 2018). Cole Park was located directly in front of a stormwater runoff drain on the western shoreline of CCB. The stormwater drain receives inputs from ~6 km^2 of densely populated drainage area. The Canal site was located in a densely populated residential neighborhood with extensive man-made canals and little connectivity to surrounding waters. The closest connected body of water is the Laguna Madre, and freshwater inputs were in the form of overland runoff from yards and roadways.

Field Sampling

All sites were visited following the same temporally variable schedule: monthly in December, January, and February; biweekly in October (2017), November, and March through August; weekly in September and October (2016 and 2018). This resulted in a total of 59 sampling events spanning 27 months. Sampling during each event began no earlier than 830 am and concluded no later than 200 pm, with most sampling events occurring between 900 am and 1230 pm. There is a limited influence of tidal exchange due to relatively small diurnal tidal range on this part of the Gulf of Mexico coastline (Ward 1997). Surface water hydrographic data (temperature, conductivity (salinity), pH, and dissolved oxygen) were collected using a calibrated YSI ProPlus multiparameter sonde (YSI Inc., Yellow Springs, OH). Light attenuation was measured at each site with a Secchi disc; however, there were instances where the current was too swift for the disc to descend at a near 90° angle (Packery Channel, $n = 33$ out of 59 and Oso Inlet, $n = 7$ out of 59). Water samples were collected from the top 15 cm of the water surface and transported to the lab in acid-washed amber polycarbonate bottles for further processing. Water for micro- and nanophytoplankton enumeration (500 mL) was stored at ambient temperature and samples for nutrient chemistry, chlorophyll *a* analysis, and picophytoplankton cell counts were collected as field duplicates (1-L each) and stored on ice (~0 °C) until return to the lab (< 3 h).

Laboratory Processing

Prior to sample processing, the collection bottles were gently inverted to homogenize the water and suspended

materials. Water for micro- and nanophytoplankton enumeration was gently poured into 50 mL conical vials and fixed with acidified Lugol's solution to a final concentration of 1% and stored at room temperature in the dark. Water for dissolved nutrient (ammonium, nitrate plus nitrite, orthophosphate, silicate, dissolved organic carbon, and total dissolved nitrogen) quantification was filtered through pre-combusted (4 h at 450 °C) Ahlstrom GF/F filters into HDPE bottles. For chlorophyll *a* quantification, a known volume of water was gently filtered (≤ 5 mm Hg) through 25 mm Whatman GF/F filters. For picophytoplankton quantification, site water was fixed with 50% glutaraldehyde to a final concentration of 1%. For each variable, duplicate samples were processed. Following sample processing described above, all samples were immediately stored at −20 °C until analysis.

Phytoplankton Enumeration

Micro- and nanophytoplankton were counted by following the Utermöhl method on an Olympus IX71 inverted microscope at 200× magnification. The volume settled for each sample was variable based on chlorophyll *a* concentration and the quantity of suspended solids noted during live screens. The total volume settled for each sample ranged from 0.5 to 20 mL. Small settling volumes were associated with high chlorophyll *a* or high suspended sediment loads, whereas large settling volumes were associated with low chlorophyll *a* and low suspended sediment loads. All samples were settled overnight (> 12 and ≤ 24 h), allowing at least 1 h of settling time per mL of sample settled. Picophytoplankton was counted using an Accuri C6 Plus flow cytometer with the CSampler Plus adapter (Beckton Dickinson, San Jose, CA). Instrument QC was performed daily following manufacturer protocol prior to sample preparation. Samples were thawed at 0 °C in the dark and gently filtered across 20 µm Nytex® mesh to remove large cells and particulate matter. All samples were run on the fast setting, with a flow rate of 66 µL min^{-1} and a core size of 22 µm. The auto-sampler was set to agitate the sampling plate and rinse the sample input port before and after each sample was analyzed. Additionally, polystyrene beads of known size (3.3 µm) were run at the same settings to ensure that only appropriate size ranges of cells were counted. Biovolumes were estimated for micro-, nano-, and picophytoplankton using the associated geometric shapes at the lowest taxonomic resolution recorded during counting (Sun and Liu 2003). Picophytoplankton shape and size were not directly measured and were estimated to be spherical at 1.5 µm and 2.5 µm diameters for picocyanobacteria and picoeukaryotes, respectively.

Nutrients

Inorganic nutrient samples were thawed to room temperature and then analyzed on a Seal QuAAtro autoanalyzer. Standard curves with five different concentrations were run daily at the beginning of each run. Fresh standards were made prior to each run by diluting a primary standard with low nutrient surface seawater. Deionized water (DIW) was used as a blank, and DIW blanks were run at the beginning and end of each run, as well as after every 8–10 samples to correct for baseline shifts. Method detection limits were 0.02 µM for nitrate plus nitrite (NO_x) and ammonium (NH_4^+), and < 0.01 µM for orthophosphate (PO_4^{3-}) and silicate (SiO_4). Dissolved inorganic nitrogen (DIN) was calculated as the sum of NH_4^+ and NO_x. Samples for dissolved organic carbon (DOC) and total dissolved nitrogen (TDN) were thawed to room temperature and analyzed using the High Temperature Catalytic Oxidation method on a Shimadzu TOC-Vs analyzer with nitrogen module. Standard curves were run twice daily using a DIW blank and five concentrations of either acid potassium phthalate solution or potassium nitrate for DOC and TDN, respectively. Three to five subsamples were taken from each standard and water sample and injected in sequence. Reagent grade glucosamine was used as a laboratory check standard and inserted throughout each run, as were Certified Reference Material Program (CRMP) deepwater standards of known DOC/TDN concentration. Mean daily CRMP DOC and TDN concentrations were 44.2 ± 2.7 µmol L^{-1} and 31.9 ± 2.4 µmol L^{-1}, respectively. Dissolved organic nitrogen (DON) was determined by subtracting dissolved inorganic nitrogen (NH_4^+ and NO_x) from TDN.

Accessory Data Collection

Daily precipitation totals and mean daily wind speeds were downloaded from the NOAA National Climate Data Center for the Corpus Christi Naval Air Station (station code USW00012926; accessed 4/6/2020). The precipitation data was used to assign each sampling event a value representing days since rainfall > 2.54 mm (DSR). Where rainfall and sampling events overlapped, a value of 0 was assigned.

Data Analysis

All raw data and associated R code are available at https://doi.org/10.7266/NCPYG0DH. Data analyses were performed in R v 3.5.2 and PRIMER v7. Prior to statistical analyses, NO_x ($n = 70$) and PO_4^{3-} ($n = 3$) measurements that were below the detection limit were coded as the method detection limits of 0.02 µM and 0.005 µM, respectively. There was one instance where calculated DON was negative, and the value was coded as 0. DIN:DIP was calculated

as DIN divided by PO_4^{3-}, and DIN:Si was calculated as DIN divided by SiO_4. Where averages are presented (i.e., site or season averages), DIN:DIP and DIN:Si were calculated with average DIN and average PO_4^{3-} and SiO_4, respectively. The error for the ratios was then calculated using the formula

$$(\mathrm{DIN}/\mathrm{var}) \times \sqrt{(\mathrm{sd\ DIN}/\mathrm{DIN})^2 + (\mathrm{sd\ var}/\mathrm{var})^2}$$

where sd indicates standard deviation, DIN is mean DIN, and var is either the mean of PO_4^{3-} or SiO_4 for the DIN:DIP and DIN:Si ratios, respectively. For the following analyses, seasons are defined as follows: spring = March, April, and May; summer = June, July, and August; fall = September, October, and November; and winter = December, January, and February.

Two-way ANOVAs with site and season were used to explore spatial and seasonal patterns in individual environmental and biological variables (stats v 3.5.2; R Core Team 2019). For environmental variables, where sampling was conducted on sub-monthly time scales, data were averaged by sampling month at each site prior to conducting ANOVAs to achieve a more balanced dataset. For each variable examined, the interaction term for site and season was used as an explanatory factor to test for a significant interaction between factor levels. If there was no significant interaction, one-way ANOVAs were used to test for site and season differences individually, without regard to the other factor (stats v 3.5.2; R Core Team 2019). If a significant interaction was detected, one-way ANOVAs were used to test for site differences within each level of season, and vice versa. Each one-way ANOVA was tested for assumptions of normality (Shapiro–Wilk test) and homoscedasticity of variance (Brown-Forsythe Levene test). If necessary, terms to address heteroscedasticity were included in the ANOVA models (nlme v. 3.1–145; Pinheiro et al. 2020). Multiple comparison procedures with Tukey's contrasts were then used to compare all possible season and site pairs with a Westfall correction applied to the *p*-values (multcomp v 1.4–12; Hothorn et al. 2008). Corrected *p*-values were compared to $\alpha = 0.1$ to account for introduction of Type II error (Quinn and Keough 2002).

Due to an exceptional outlier event in phytoplankton biovolume associated with the occurrence of a short-lived *K. brevis* red tide (one event 10/14/2016), median values of phytoplankton biovolume as well as the biovolume of major taxonomic groups were reported instead of means as they were more representative of overall site and season conditions. The Kruskal-Wallis rank-based non-parametric test is better suited for comparing conditions among factor levels when there are a few strong outliers (stats v. 3.5.2; R Core Team 2019; Quinn and Keough 2002) and was therefore used to compare sites and seasons for phytoplankton biovolume, and the biovolume of diatoms, dinoflagellates, picocyanobacteria, and picoeukaryotes. To determine if there was a significant interaction between site and season, the five datasets were rank-transformed and an ANOVA with the interaction term between site and season was used as an explanatory variable, since the Kruskal-Wallis test is only for one-way designs (stats v. 3.5.2; R Core Team 2019; Quinn and Keough 2002). Where there was no significant interaction between site and season, one-way Kruskal-Wallis tests were performed with site and season as explanatory variables individually (stats v. 3.5.2; R Core Team 2019). Where there was significant interaction between site and season one-way Kruskal-Wallis tests, comparing sites were performed at each level of season, and vice versa. Multiple comparison procedures with Tukey's contrasts were then used to compare all possible season and site pairs with a Holm correction applied to the *p*-values. Corrected *p*-values were compared to $\alpha = 0.1$ to account for introduction of Type II error (Quinn and Keough 2002).

To assess seasonal and spatial environmental variability, principal component analyses (PCA) were conducted in PRIMER v7 (Clarke and Gorley 2015). One PCA was conducted including all sampling events across all sites to characterize temporal and spatial variability. Salinity, temperature, dissolved oxygen, pH, DON, NO_x, NH_4^+, SiO_4, PO_4^{3-}, DIN:DIP, DIN:Si, and DSR were included in the PCAs, and all variables were normalized prior to analysis. Principal components to be interpreted were selected following the Kaiser Guttman Criterion (Borcard et al. 2011) To quantify relationships between temperature and salinity and nutrient parameters, pairwise Kendall's Tau correlations were conducted on untransformed data (stats v. 3.5.2; R Core Team 2019).

To quantify the relationships among environmental factors and phytoplankton biovolume, pairwise Kendall's Tau correlations were conducted on untransformed data (stats v. 3.5.2; R Core Team 2019). Pairwise Kendall's Tau correlations between environmental variables and diatom, dinoflagellate, picocyanobacteria, and picoeukaryote biovolume were conducted on untransformed data (stats v. 3.5.2; R Core Team 2019). These four taxonomic groups, on average, comprised approximately 90% of the phytoplankton community in the CCB system and were considered important contributors to the phytoplankton community across nearly all sampling events.

Results

Environmental Dynamics

Environmental conditions in the CCB system varied along two main principal component (PC) axes, one of which was generally representative of stochastic processes

(PC1) and one of which was generally representative of seasonal variability (PC2) (Fig. 3). Eigenvalues for each PC and variable eigenvectors can be found in electronic supplemental materials (Tables S1 and S2). The variables that most strongly contributed to the creation of the stochastic processes axis were NO_x, salinity, and PO_4^3 (Fig. S3). Moderate contributions to the creation of this axis were also seen for SiO_4, DOx, temperature, NH_4^+, and DSR, with approximately 22% of the dataset variability explained by this PC. The generally inverse relationship between nutrients and salinity, and between salinity and DSR can also be seen in Fig. 4, and the results of pairwise Kendall's Tau correlations (Tables S4–S6). The spread of sampling events along PC1 indicated that the influence of

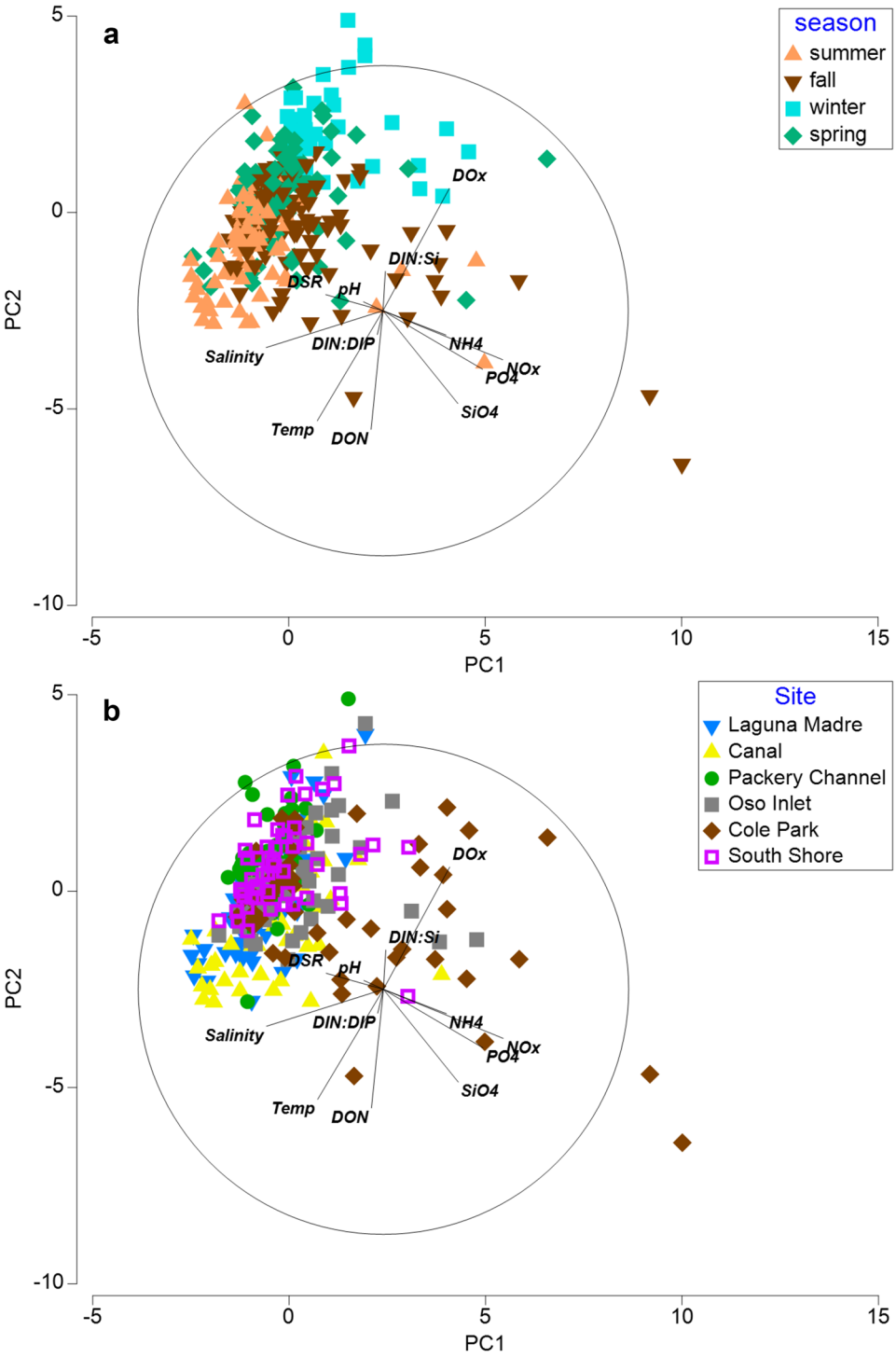

Fig. 3 PCA plot with sampling events coded by sampling site. Variable abbreviations are as follows: Temp, temperature; DOx, dissolved oxygen; DON, dissolved organic nitrogen; NOx, nitrate + nitrite; PO4, phosphate; NH4, ammonium; SiO4, silicate; DSR, days since rainfall > 2.54 mm. All other variables are as displayed. Panel **a** shows sampling events coded by season and panel **b** shows sampling events coded by site. Figure 3 was created using PRIMER-E software

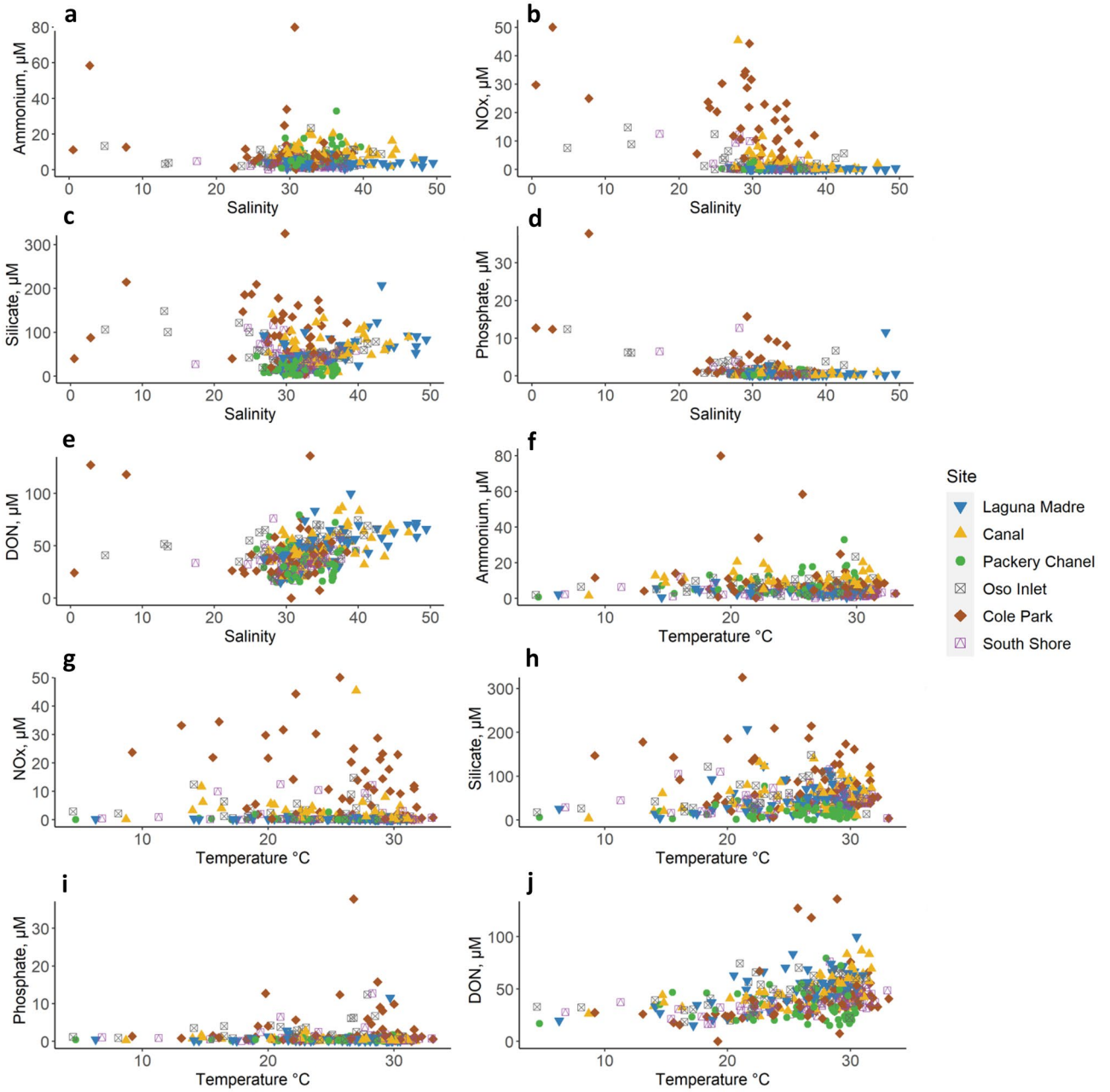

Fig. 4 Scatter plots comparing salinity (**a**–**e**) and temperature (**f**–**j**) to ammonium (**a**, **f**), nitrate + nitrite (**b**, **g**), silicate (**c**, **h**), phosphate (**d**, **i**), and DON (**e**, **j**). Figure 4 was created using the R statistical software package and MSOffice

stochastic processes was most pronounced during the fall season (Fig. 3a) and at the Cole Park site (Fig. 3b), though other seasons and sites demonstrated some degree of variability along this axis. Given the seasonal variability in the total number of precipitation events producing > 2.54 mm, the mean volume of precipitation documented over the course of this study (Table 1), and the proximity of the Cole Park site to a stormwater runoff drain, the PCA was able to accurately represent seasonal and spatial variability in precipitation-driven stochasticity in the CCB system.

The seasonal variability captured in PC2 was most strongly related to DOx, DON, temperature, and SiO_4 (Fig. S3). Moderate contributions to the creation of this PC were also seen for the variables PO_4^{3-}, NO_x, DIN:Si, and salinity, with approximately 19% of the dataset variability explained by this PC. The generally positive relationship between DON and temperature can also be seen in Fig. 4 and the results of pairwise Kendall's Tau correlations (Tables S4–S6). The spread of sampling events along PC2 supports the conclusion that this axis is representative of seasonal

Table 1 Total number of rainfall events producing greater than 2.54 mm of rain, total volume of rainfall (mm), and mean volume of rainfall (mm) for each season from August 2016 through October 2018

Season	Number of rainfall events	Total volume of rainfall events	Mean volume of rainfall events
Spring	18	234.95	7.34
Summer	19	364.24	12.56
Fall	35	943.61	15.99
Winter	16	188.72	4.29

processes driving environmental variability, with summer samples associated with higher temperatures and lower DOx compared to winter samples (Fig. 3a). There is also evidence of some spatial variability captured by PC2 (Figs. 3b and 5). The Laguna Madre and Canal sites, characterized by larger distances from freshwater sources and a lower degree of overall connectivity with surrounding bodies of water, demonstrated higher temperatures and DON concentrations and lower DOx, especially during summer months, as seen in the generally negative PC2 scores associated with these sites (Fig. 5). Though difficult to see in the PCA due to overlapping sampling events, the Packery Channel site tended to be characterized by lower temperatures and higher DOx than other sites, especially during summer months (Fig. 5). Similar to the observed seasonal and spatial variability in stochasticity observed along PC1, these results indicate that spatial variability may influence the seasonal signal in environmental conditions observed.

Results from one-way ANOVAs comparing nutrient concentrations among seasons and sites support the observed patterns in the PCA described above (Table 2). *p*-values for all pairs comparisons presented in Table 2 can be found in electronic supplemental material (Table S7). Additionally, there was a significant interaction found between site and season for the variables DON, PO_4^{3-}, SiO_4, and DIN:Si (Table 2), providing further evidence for the role of spatial variation among sites influencing observed seasonal patterns in environmental conditions. Results of Kendall's Tau pairwise correlations between salinity and temperature and NO_x, NH_4^+, PO_4^{3-}, SiO_4, DON, and DSR at the site-specific level (Tables S5 and S6) and scatter plots of the same variables (Fig. 4) provide a more detailed look at how environmental conditions at each site respond to seasonal and stochastic processes.

At the level of the CCB system, temperature was significantly inversely related to NO_x and PO_4^{3-}, positively related to DON and SiO_4, and unrelated to DSR and NH_4^+ (Fig. 4; Table S4). At the site-specific level of resolution, temperature was also inversely correlated with NO_x at the Laguna Madre, Canal, Oso Inlet, and Cole Park sites, and with PO_4^{3-} at the Canal and Oso Inlet sites (Table S6). In contrast, a positive relationship was found between temperature and PO_4^{3-} at the Packery Channel site. Positive relationships between temperature and DON were found across all sites other than Packery Channel, supporting the strong relationship between temperature and DON seen in the PCA. In contrast, SiO_4 only demonstrated a significant positive relationship with temperature and the Laguna Madre site, though at the Canal and Oso Inlet sites this relationship was only borderline non-significant (*p*-values of 0.084 and 0.085, respectively).

At the level of the CCB system, salinity was significantly inversely related to NO_x and PO_4^{3-}, positively related to DON and DSR, and unrelated to NH_4^+ (Fig. 4; Table S5). The relationship between salinity and SiO_4 was positive, but

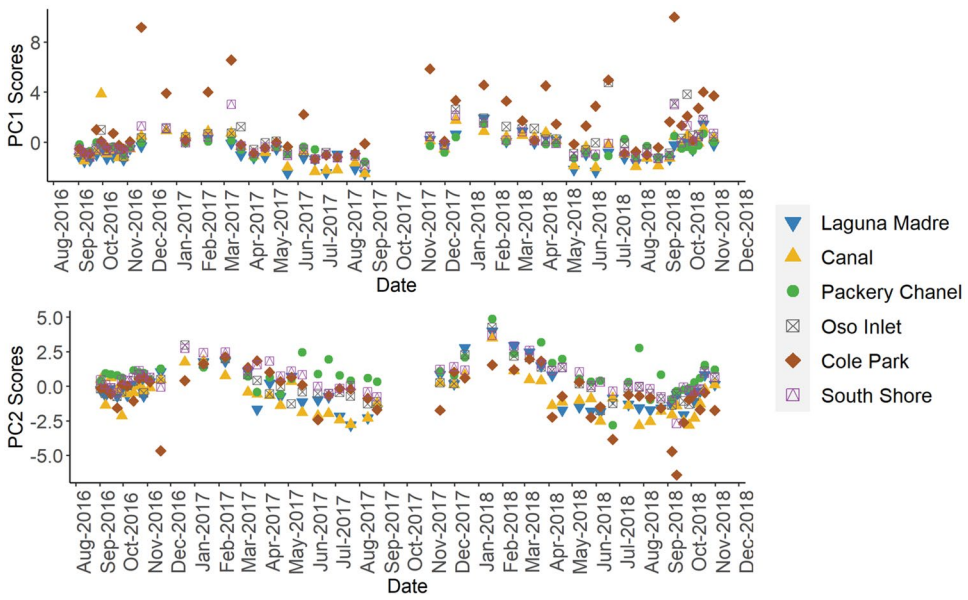

Fig. 5 Principal component scores for each sampling event plotted over time and coded by site to better resolve the spatial variability associated with stochasticity and seasonality. Figure 5 was created using the R statistical software package and MSOffice

Table 2 Mean and (std deviation) of temperature, salinity, and selected nutrient parameters across sites and seasons

	Sites						Seasons			
	Laguna Madre	Canal	Packery Channel	Oso Inlet	Cole Park	South Shore	Spring	Summer	Fall	Winter
Temperature (°C)	23.95 (6.01)	24.43 (6.17)	23.88 (5.95)	23.49 (6.89)	24.55 (6.23)	24.34 (6.62)	23.38 (2.52)^{c}	30.11 (1.08)^{a}	26.34 (2.34)^{b}	14.32 (4.36)^{d}
Salinity	35.71 (5.21)^{a}	34.87 (4.42)^{a,b}	32.72 (2.81)^{b,c}	31.60 (4.72)^{c,d}	29.68 (5.11)^{d}	31.61 (2.99)^{c,d}	33.65 (5.47)^{b}	36.31 (4.28)^{a}	30.81 (3.58)^{c}	29.80 (1.85)^{c}
NH_4^+ (µM)	3.94 (1.82)^{c}	9.18 (4.07)^{a}	7.43 (4.66)^{a,b}	6.37 (3.29)^{b}	11.15 (15.14)^{a,b}	3.83 (2.39)^{c}	7.02 (3.47)^{a}	7.08 (4.47)^{a}	5.29 (4.93)^{b}	9.29 (13.33)^{a,b}
NO_x (µM)	0.27 (0.20)^{e}	2.59 (2.82)^{b}	0.38 (0.30)^{d,e}	2.02 (2.87)^{b,c}	12.69 (10.66)^{a}	1.34 (2.45)^{c,d}	2.47 (4.79)^{a,b}	1.75 (4.43)^{b}	3.44 (6.18)^{a,b}	5.67 (9.24)^{a}
DON* (µM)	46.54 (15.33)	45.63 (15.05)	33.55 (11.49)	44.76 (12.07)	36.67 (17.79)	34.89 (8.73)	36.03 (12.72)	48.81 (14.81)	44.5 (11.89)	28.58 (9.85)
PO_4^{3-}* (µM)	0.64 (1.13)	0.68 (0.41)	0.52 (0.29)	1.72 (1.92)	2.55 (3.46)	0.83 (0.99)	1.09 (1.25)	1.11 (2.37)	1.44 (2.24)	0.94 (1.01)
SiO_4* (µM)	49.61 (29.30)	52.68 (28.71)	16.45 (11.52)	46.72 (21.60)	86.00 (55.65)	40.22 (22.01)	52.31 (44.89)	49.56 (30.09)	52.08 (31.16)	39.56 (43.12)
DIN:DIP	6.55 (11.89)^{a,b,c}	17.31 (13.20)^{a}	14.96 (12.15)^{a}	4.88 (6.05)^{c}	9.33 (14.61)^{a,b}	6.22 (8.95)^{b,c}	8.73 (11.39)^{a}	7.99 (18.41)^{a}	6.07 (11.86)^{b}	15.94 (24.49)^{a}
DIN:Si*	0.09 (0.07)	0.22 (0.16)	0.47 (0.43)	0.18 (0.13)	0.28 (0.29)	0.13 (0.13)	0.18 (0.19)	0.18 (0.19)	0.17 (0.23)	0.38 (0.59)

An asterisk (*) denotes a significant interaction between site and season. Letters indicate the results of a one-way ANOVA, with a > b > c > d > e

with a *p*-value of 0.050 can only be considered a borderline result. At the site-specific level of resolution, salinity was also inversely correlated with NO_x at all sites other than Packery Channel, and with PO_4^{3-} at the Packery Channel, Oso Inlet, Cole Park, and South Shore sites. These results demonstrate a generally widespread relationship between salinity and nutrient inputs. Significant positive relationships between salinity and DON were found at the Laguna Madre, Canal, Oso Inlet, and South Shore sites, though at Cole Park the relationship was borderline (*p*-value = 0.053). At all sites, a positive correlation was found between salinity and DSR, indicating that salinity may be an acceptable proxy for precipitation and precipitation-driven nutrient inputs in this system. Lastly, the borderline relationship observed for salinity and SiO_4 at the system-wide level of resolution is likely explained by observed variability in the results of the site-specific correlations. SiO_4 was found to positively correlate with salinity at the Laguna Madre and Canal sites, whereas an inverse correlation was observed at the Cole Park site and no significant relationship was observed at the remaining three sites.

Phytoplankton Population Dynamics

Phytoplankton biovolume varied seasonally and demonstrated a unimodal pattern with the highest biovolume observed during spring and summer and the lowest biovolume observed during fall and winter (Fig. 6). *p*-values and estimated differences for each pairwise comparison for the Kruskal-Wallis results presented here can be found in the electronic supplemental material (Table S8). Spatial variability was also observed with the highest biovolume observed at the Canal, Packery Channel, Oso Inlet, and South Shore sites, intermediate biovolume observed at the Laguna Madre site, and the lowest biovolume observed at the Cole Park site (Fig. 6; Table S8). On average, diatoms were the largest contributor to phytoplankton biovolume, accounting for approximately 34.0% of total phytoplankton biovolume, followed by dinoflagellates (27.7%), picocyanobacteria (20.3%), and picoeukaryotes (8.1%) (Figs. 7 and 8). Given that these four groups of phytoplankton accounted for approximately 90% of the entire community, further statistical analyses were focused on these four groups.

Patterns of seasonal and spatial variability in the biovolume of the four major taxonomic groups of phytoplankton were also observed (Table 3). Associated *p*-values and estimated differences for each pairwise comparison can be found in the electronic supplemental material (Table S8). Diatoms, picocyanobacteria, and picoeukaryotes all demonstrated higher median biovolume during the spring. Diatoms and picoeukaryotes demonstrated a significant

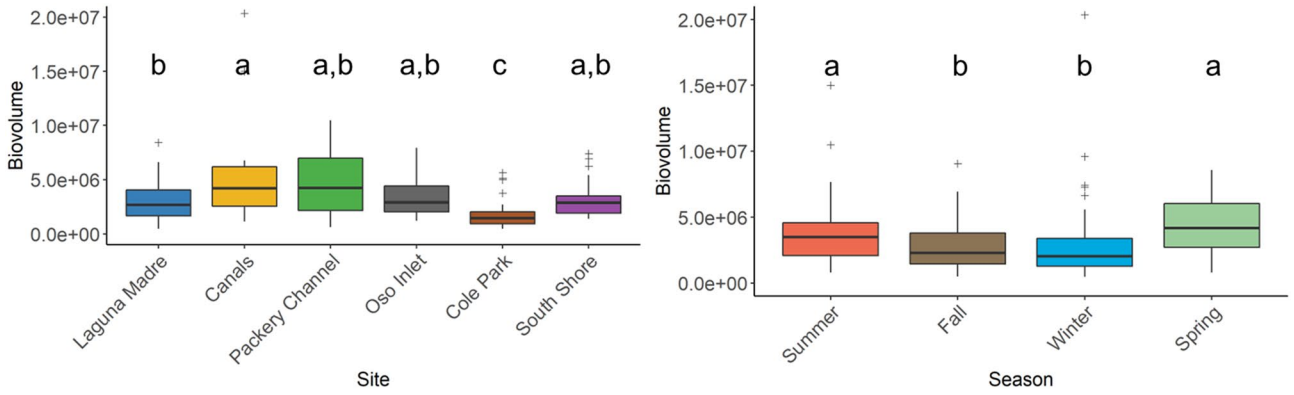

Fig. 6 Boxplots of phytoplankton biovolume ($\mu m^3\ mL^{-1}$) across sites (**a**) and seasons (**b**). Thick line represents median values and outliers are represented by (+). There is a single outlier not shown on these graphs that occurred at Cole Park during the fall of 2016 (10/14/2016) associated with a *K. brevis* red tide. The total biovolume of that event was $1.94 \times 10^8\ \mu m^3\ mL^{-1}$. Figure 6 was created using the R statistical software package and MSOffice

decrease in median biovolume from spring into summer, whereas there was no difference in the median biovolume of picocyanobacteria between these seasons. Median picoeukaryote biovolume also demonstrated a significant decline from summer into fall, and from fall into winter. Similarly, median picocyanobacteria biovolume began to decline from summer into fall, and from fall into winter. In contrast, median diatom biovolume in the fall was similar to that in the summer and demonstrated a significant increase from fall into winter.

Spatially, Cole Park consistently demonstrated the lowest median biovolume across major taxonomic groups, similar to the finding of the lowest overall phytoplankton biovolume at this site (Table 3). Picoeukaryotes and picocyanobacteria both demonstrated higher median biovolume at the Canal and Oso Inlet sites, in contrast to diatoms where the highest median biovolume was observed at the Packery Channel site. For all three groups, intermediate biovolume was found at the South Shore and Laguna Madre sites.

There was a significant interaction between site and season when comparing dinoflagellate biovolume. As such, all possible pairs comparisons of season were conducted within each level of site, and vice versa. All sites other than Packery Channel demonstrated seasonal variability in the biovolume of dinoflagellates (Table 4; Fig. 7). *p*-values and estimated differences of pairwise comparisons associated with these analyses can be found in the electronic supplemental material (Tables S9 and S10). The most pronounced seasonal variability was observed at the Laguna Madre site with the highest median biovolume observed during the summer, followed by fall, and then winter and spring. At the Canal site, the only difference observed was between summer (higher) and winter (lower). At the Oso Inlet site, median dinoflagellate

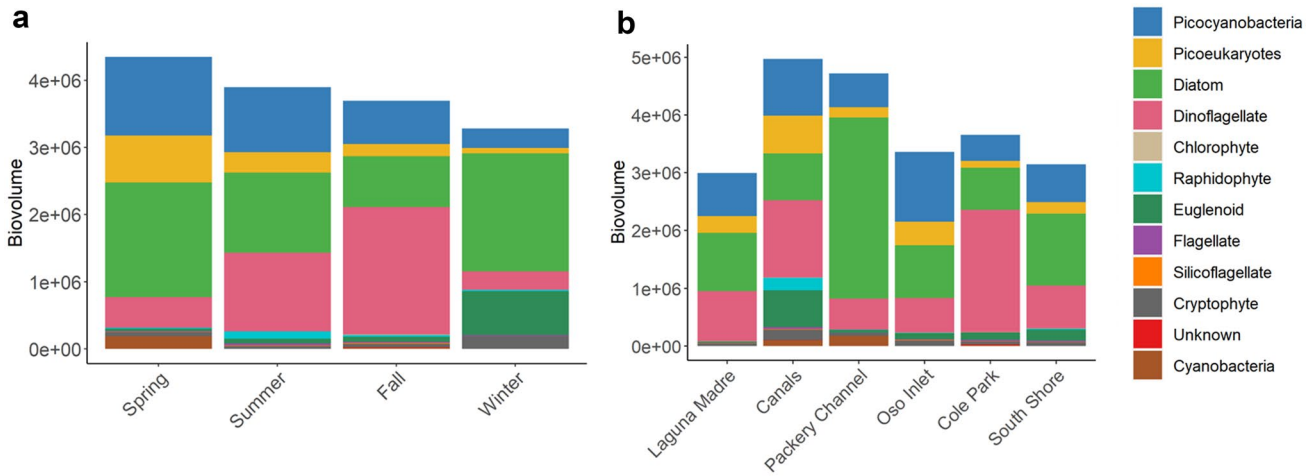

Fig. 7 Stacked bar graphs of median phytoplankton biovolume ($\mu m^3\ mL^{-1}$) coded by major taxonomic group. Panel **a** represents seasonal medians and panel **b** represents site-specific medians. Figure 7 was created using the R statistical software package and MSOffice

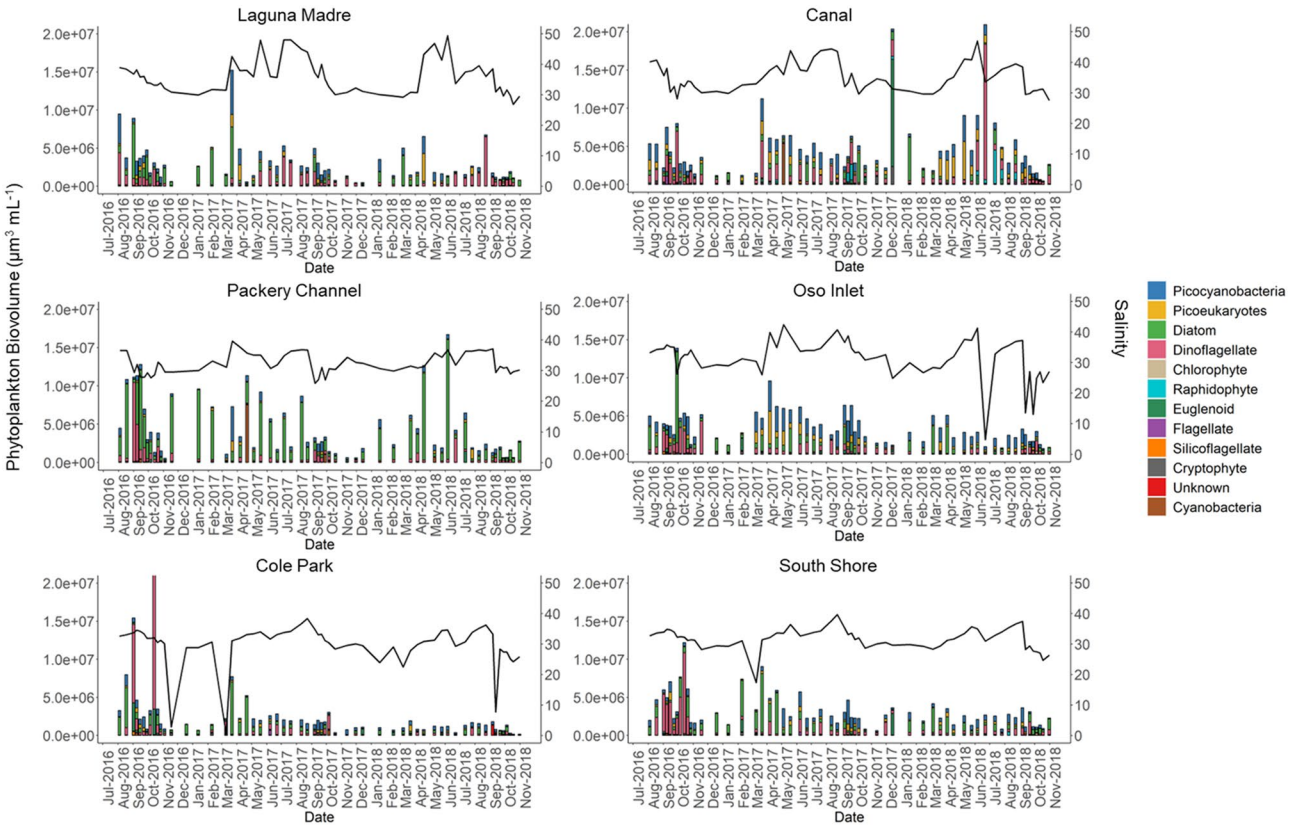

Fig. 8 Temporal variability in phytoplankton biovolume (μm^3 mL^{-1}) and major group contribution at all sites studied. Black line represents salinity. At Cole Park, the sampling event with phytoplankton biovolume greater than the scale of the plot was on 10/14/2016 associated with a *K. brevis* red tide. The total biovolume was 1.94 × 10^8 μm^3 mL^{-1}. Figure 8 was created using the R statistical software package and MSOffice

biovolume in the fall was significantly higher than in the winter and spring, whereas at the Cole Park site, summer and fall median biovolume were both significantly higher than winter. Lastly, at the South Shore site, median dinoflagellate biovolume was significantly higher in the fall than in the spring. Despite the site-specific patterns in seasonal dinoflagellate biovolume, the general pattern indicated that warmer seasons (summer and fall) typically demonstrated median higher biovolume than cooler seasons (winter and spring).

Spatial patterns in median dinoflagellate biovolume at each level of season were similarly variable (Table 4). During the summer, the Laguna Madre and Canal sites demonstrated significantly higher dinoflagellate biovolume than the Oso Inlet, Cole Park, and Packery Channel sites. The Laguna Madre also demonstrated significantly higher biovolume than the South Shore site, though there was no difference between the latter and the Canal site. During the fall, winter, and spring, there were fewer site-specific differences in median dinoflagellate biovolume. During the fall, the only observed difference was between the Oso Inlet (higher) and Cole Park (lower) sites, and during the winter, the only observed differences were between the Canal and South Shore sites (higher) and the Cole Park site (lower). Lastly, during the spring, the Canal site demonstrated significantly higher median dinoflagellate biovolume than the Laguna Madre, Oso Inlet, and Cole Park sites. Taken together, these results indicate that, in general, the Laguna Madre, Canal, and Oso Inlet sites tended to exhibit higher median dinoflagellate biovolume than other sites, regardless of season.

The remaining ~10% of the phytoplankton community was comprised of euglenoids (5.0%), cryptophytes (2.2%), cyanobacteria (1.3%), raphidophytes (1.1%), small unidentified flagellates (0.4%), silicoflagellates (0.2%), chlorophytes (0.1%), and unclassified organisms (0.1%). Despite the relatively low overall contributions of euglenoids, cyanobacteria, and raphidophytes, there were occasions where these groups contributed a larger percentage to the phytoplankton community (Fig. 8). Peaks in euglenoid biovolume (≥ 50% of total biovolume) occurred on 2/9/2017 (Oso Inlet),

Table 3 Median and (range) of biovolume ($\mu m^3 L^{-1} \times 10^5$) of the four most abundant major taxonomic groups across sites and seasons

Seasons	Diatoms	Picocyanobacteria	Picoeukaryotes
Summer	4.49 [b] (0.15–156.47)	8.11 [a] (1.26–39.47)	1.86 [b] (0.17–14.60)
Fall	3.67 [b] (0.00–118.89)	4.79 [b] (0.16–38.97)	0.90 [c] (0.00–12.14)
Winter	9.82 [a] (0.15–90.10)	1.65 [c] (0.13–15.93)	0.52 [d] (0.08–5.01)
Spring	7.90 [a] (0.43–113.37)	7.40 [a] (1.43–58.06)	2.96 [a] (0.42–49.69)
Sites	**Diatoms**	**Picocyanobacteria**	**Picoeukaryotes**
Laguna Madre	4.60 [b,c] (0.26–71.63)	4.55 [c] (0.16–58.06)	1.06 [c] (0.04–36.25)
Canal	3.71 [b,c] (0.15–56.88)	7.39 [a,b] (0.32–34.25)	3.30 [a] (0.13–49.69)
Packery Channel	12.66 [a] (0.88–156.47)	5.02 [c] (0.36–44.80)	1.12 [c] (0.04–13.43)
Oso Inlet	4.27 [b,c] (0.46–118.89)	12.24 [a] (0.17–39.75)	2.29 [a,b] (0.08–42.43)
Cole Park	3.00 [c] (0.00–68.68)	3.93 [c] (0.18–35.31)	0.71 [d] (0.04–8.05)
South Shore	6.14 [b] (0.28–77.14)	6.00 [b,c] (0.12–31.47)	1.29 [b,c] (0.00–10.51)

Results of one-way Kruskal-Wallis ANOVAs comparing differences among sites and seasons denoted by superscript letters, with the order a > b > c > d

12/14/2017 (Canal, Cole Park, South Shore), and 2/15/2018 (Cole Park). Cyanobacteria and raphidophyte peaks occurred less frequently, with two cyanobacteria peaks occurring on 4/21/2017 (Packery Channel) and 5/5/2017 (Canal) and only a single peak in raphidophyte biovolume on 7/12/2018 (Canal).

Table 4 Median and (range) of biovolume ($\mu m^3 L^{-1} \times 10^5$) of dinoflagellates at each level of season with site and each level of site within season

Season comparisons at each level of site						
Seasons	Laguna Madre	Canal	Packery Channel	Oso Inlet	Cole Park	South Shore
Summer	15.25 [a] (2.10–64.71)	11.85 [a] (3.39–177.33)	2.76 (0.19–31.51)	4.47 [a,b] (0.49–17.66)	3.00 [a] (0.10–12.83)	4.65 [a,b] (0.02–23.46)
Fall	5.50 [b] (0.05–22.05)	5.90 [a,b] (2.01–67.04)	3.60 (0.27–103.21)	7.19 [a] (0.21–42.98)	2.44 [a] (0.06–1856.92)	6.15 [a] (0.35–106.30)
Winter	1.31 [c] (0.00–3.73)	4.18 [b] (0.31–21.64)	2.40 (1.65–3.33)	1.65 [b] (0.30–3.15)	0.49 [b] (0.15–2.82)	3.78 [a,b] (1.04–4.14)
Spring	1.46 [c] (0.02–18.99)	5.27 [a,b] (1.65–48.36)	1.73 (0.48–11.02)	1.16 [b] (0.20–6.97)	1.43 [a,b] (0.38–14.93)	2.18 [b] (0.10–17.33)
Site comparisons at each level of season						
Seasons	Laguna Madre	Canal	Packery Channel	Oso Inlet	Cole Park	South Shore
Summer	15.25 [a] (2.10–64.71)	11.85 [a,b] (3.39–177.33)	2.76 [c] (0.19–31.51)	4.47 [c] (0.49–17.66)	3.00 [c] (0.10–12.83)	4.65 [b,c] (0.02–23.46)
Fall	5.50 [a,b] (0.05–22.05)	5.90 [a,b] (2.01–67.04)	3.60 [a,b] (0.27–103.21)	7.19 [a] (0.21–42.98)	2.44 [b] (0.06–1856.92)	6.15 [a,b] (0.35–106.30)
Winter	1.31 [a,b] (0–3.73)	4.18 [a] (0.31–21.64)	2.40 [a,b] (1.65–3.33)	1.65 [a,b] (0.30–3.15)	0.49 [b] (0.15–2.82)	3.78 [a] (1.04–4.14)
Spring	1.46 [b] (0.02–18.99)	5.27 [a] (1.65–48.36)	1.73 [a,b] (0.48–11.02)	1.16 [b] (0.20–6.97)	1.43 [b] (0.38–14.93)	2.18 [a,b] (0.10–17.33)

Results of one-way Kruskal-Wallis ANOVAs comparing differences among sites within seasons and vice versa denoted by superscript letters, with the order a > b > c

Table 5 Environmental variables found to be significantly ($p < 0.05$) related to phytoplankton biovolume based on pairwise Kendall's Tau correlations

Variables	Correlation coefficient	*p*-value
NOx	−0.168	< 0.001
PO_4^{3-}	−0.118	0.001
SiO_4	−0.098	0.006
DSR	0.096	0.017
Temperature	0.125	< 0.001
pH	0.196	< 0.001
Salinity	0.243	< 0.001

Days since rainfall > 2.54 mm is abbreviated as DSR

Phytoplankton-Environment Relationships

At the system-wide level, phytoplankton biovolume was inversely correlated with NO_x, PO_4^{3-}, and SiO_4, and positively correlated with DSR, temperature, pH, and salinity (Table 5). For each of the four major taxonomic groups examined here, there were some similarities to the patterns observed for total community biovolume as well as among groups. All correlations between major taxonomic group biovolume and NO_x were inverse, similar to that observed for the whole community biovolume (Table 6). Other variables found to correlate with the biovolume of all four major taxonomic groups were temperature, SiO_4, DON, DOx, and DIN:Si, though the direction of the relationship was variable among groups.

Temperature, DON, and SiO_4 were all positively correlated with dinoflagellate, picocyanobacteria, and picoeukaryote biovolume, but inversely correlated with diatom biovolume. Similarly, DIN:Si and DOx were positively correlated with diatom biovolume and inversely correlated with dinoflagellate, picocyanobacteria, and picoeukaryote biovolume. Of the remaining variables, average daily wind speed was only found to be correlated with diatoms (positive) and dinoflagellates (inverse), PO_4^{3-} was only found to be correlated with diatoms and picoeukaryotes (both inverse), salinity was found to be positively correlated with all groups other than diatoms (no relationship observed), and lastly DSR was only correlated with picocyanobacteria and picoeukaryotes (both positive).

Table 6 Environmental variables found to be significantly ($p < 0.05$) related to diatom, dinoflagellate, picocyanobacteria, and picoeukaryote biovolume based on pairwise Kendall's Tau correlations

Diatoms			Dinoflagellates		
Variables	Correlation coefficient	*p*-value	Variables	Correlation coefficient	*p*-value
SiO_4	−0.365	< 0.001	DIN:Si	−0.239	< 0.001
DON	−0.208	< 0.001	DOx	−0.158	< 0.001
NOx	−0.153	< 0.001	Wind speed	−0.123	0.001
PO_4^{3-}	−0.136	< 0.001	NH_4^+	−0.123	0.001
Temperature	−0.084	0.019	NOx	−0.115	0.001
DIN:Si	0.168	< 0.001	SiO_4	0.089	0.012
DOx	0.205	< 0.001	Salinity	0.169	< 0.001
Wind speed	0.216	< 0.001	DON	0.218	< 0.001
			Temperature	0.255	< 0.001

Days since rainfall > 2.54 mm is abbreviated as DSR and dissolved oxygen is abbreviated DOx

Discussion

Corpus Christi, TX, has experienced rapid population growth and increases in urbanization, which have led to decreased freshwater inflows due to damming of the Nueces River (Montagna et al. 2009), increased demand for wastewater treatment, and increased cover of impervious surfaces (~13% increase in developed land from 2001 to 2016). Despite the large-scale urbanization and long-term decrease in freshwater inflows to CCB, a recent study found only localized eutrophication symptoms (Bugica et al. 2020). The purpose of this study was to quantify phytoplankton biovolume, community composition, and the environmental factors driving seasonal and spatial variability phytoplankton dynamics. The results of this study generally supported the hypotheses presented in the introduction. Phytoplankton biovolume and community composition demonstrated expected seasonal variability, with higher biovolume observed during spring and summer, increased importance of diatoms during the winter and spring, and increased importance of dinoflagellates during the summer and fall. Spatial variability in phytoplankton biovolume demonstrated both expected and unexpected patterns. At the anthropogenically impacted Canal site, high phytoplankton biovolume and increased importance of dinoflagellates was observed. In contrast, the anthropogenically impacted Cole Park site demonstrated generally low phytoplankton biovolume as well as generally low biovolume of each of the major taxonomic groups investigated.

Environmental Dynamics

Nutrient dynamics in the CCB system were driven by localized inputs of allochthonous nutrients and internal cycling of nutrients. NO_x and PO_4^{3-} were inversely related to salinity at most of the sites studied here (Tables S4–S6),

indicating a relationship with freshwater inflows. Proximity to freshwater inflows, however, was more influential in determining patterns in PO_4^{3-} concentrations, with no relationship observed between PO_4^{3-} and salinity at sites furthest from freshwater inflows (Laguna Madre, Canals). These findings are in line with a previous study in CCB (Turner et al. 2015) and other studies documenting NO_x as a predominantly watershed-derived nutrient (Caffrey et al. 2007; Jordan et al. 2018; Bruesewitz et al. 2015; Reyna et al. 2017; Cira et al. 2021). Increased PO_4^{3-} has also been demonstrated in urban stormwater runoff (Yang and Toor 2017) and runoff from streams impacted by human-influenced land uses (Mallin et al. 2009; Cloern 2019), supporting the dynamics observed here. Concentrations of NH_4^+ were generally unrelated to salinity and temperature (Tables S4–S6). The highest mean concentrations of NH_4^+ were observed in the spring, summer, and winter supporting the lack of a relationship with temperature. This lack of a relationship indicates that like other shallow lagoonal systems, sources of NH_4^+ were predominantly internal such as porewater, groundwater, and/or water column recycling (Douglas et al. 2021; McCarthy and Bronk 2008; Glibert et al. 2010; Reyna et al. 2017; Geyer et al. 2018; Cira et al. 2021). In the low-inflow Mission-Aransas Estuary and Florida Bay estuaries, drier conditions supported higher rates of NH_4^+ regeneration and accumulation in the water column. Additionally, Morin and Morse (1999) demonstrated that NH_4^+ release from suspended sediments can be substantial in the nearby Laguna Madre estuary. With the lowest seasonal average wind speed in the Corpus Christi region occurring during the fall, this reflects the temporal variability in NH_4^+ concentrations and a likely important role of wind-driven mixing in driving the availability of NH_4^+ to water column phytoplankton.

Temperature and salinity were positively correlated with DON at all sites other than Packery Channel indicating a strong internal mechanism for the accumulation of DON (Tables S4–S6). This pattern of increased DON during warm, high salinity periods indicates that increased phytoplankton and/or seagrass production and subsequent remineralization through degradation, combined with lack of dilution from freshwater inflows or tidal exchange with the Gulf of Mexico, are important in the accumulation of DON in CCB. Sources of SiO_4 were more variable across sites than the other nutrients examined. At Cole Park, SiO_4 was inversely related to salinity, consistent with a watershed source (Table S5), whereas other sites showed no relationship or a positive relationship (Laguna Madre, Canal). These findings indicate that while there may be a watershed source of SiO_4 associated with urban development, there are likely internal sources of regenerated SiO_4 at sites that do not receive freshwater inflows (Paudel et al. 2015; Wetz et al. 2016).

Phytoplankton Biovolume and Community Composition

Phytoplankton biovolume varied in a unimodal pattern with biovolume peaking in spring and summer, followed by a decline into fall and winter. The seasonal patterns observed were similar to those reported in other Texas estuaries (Reyna et al. 2017; Chin 2020; Cira et al. 2021) and around the globe (Pinckney et al. 1998; Cloern and Jassby 2010; Guinder et al. 2010; Baek et al. 2015; Nohe et al. 2020).

During the spring and summer, phytoplankton biovolume increased concomitant with a decrease in NO_x and PO_4^{3-}, suggestive of a drawdown effect and nutrient control upon the upper limits of phytoplankton growth (Fig. 6; Table 5). Likewise, temperature was relatively high during spring and summer, and light availability would presumably have been maximal as well. Increased temperatures and light availability have often been related to spring phytoplankton blooms across estuarine ecosystems (Sverdrup 1953; Pinckney et al. 1998; Winder and Sommer 2012; Nohe et al. 2020). Despite continued declines in ambient NO_x through spring, phytoplankton biovolume remained elevated through the summer. The high degree of nutrient regeneration typical of shallow low-inflow estuaries likely supported phytoplankton growth during this time (Pinckney et al. 2001; Glibert et al. 2010; Geyer et al. 2018). Peaks in biovolume during these seasons tended to occur following precipitation events, indicating that nutrients were a strong controlling factor. In incubation experiments conducted during 2017–2018 at the South Shore site, microzooplankton grazing rates were similar to phytoplankton growth rates while pulsed N additions elicited phytoplankton growth rates that outpaced grazing rates (Table S11; Tominack 2021), further supporting a primary role for nutrient limitation in regulating phytoplankton biovolume during these seasons.

During the fall, decreases in salinity driven by precipitation events often coincided with declines in phytoplankton biovolume despite associated nutrient inputs (see "Environmental Dynamics"). Patterns of decreased biovolume following precipitation have been observed in other Texas estuaries and have been primarily attributed to washout of phytoplankton biomass (Dorado et al. 2015; Reyna et al. 2017; Chin 2020; Cira et al. 2021). In a nutrient addition bioassay conducted during the fall of 2017, phytoplankton growth was stimulated by nitrogen additions, indicating the potential for nutrient limitation during this season (Tominack 2021). Microzooplankton grazing rates were found to approximate phytoplankton growth rates under ambient nutrient conditions (Table S11), but the net growth of phytoplankton following nitrogen additions suggests that following inputs of precipitation-derived nutrients in situ, microzooplankton grazing is likely not able to control phytoplankton growth. Therefore, in line with findings from other estuarine

systems, the lack of biomass accumulation in situ may have been related to increased hydraulic flushing and washout of phytoplankton biovolume (Roelke et al. 2013; Dorado et al. 2015; Reyna et al. 2017; Cira et al. 2021). The more pronounced declines in biovolume associated with prolonged El Niño–driven rainfall during the fall of 2018 support the role of flushing in limiting fall phytoplankton biovolume accumulation (Fig. 8).

The contrasting relationships between precipitation-derived freshwater inflow and associated nutrients and phytoplankton observed in the spring and fall were likely a result of seasonal precipitation regimes and phytoplankton community composition. During fall months, there were a total of 35 precipitation events producing greater than 2.54 mm of rain, whereas spring months experienced a total of 18 events and summer months experienced a total of 19 events (Table 1). The more frequent occurrence of precipitation during the fall may have produced a more prolonged "washout period" compared to spring and summer resulting in the lower biovolume observed during the fall. Additionally, the cooler temperatures in spring were associated with diatoms, whose relatively rapid growth rates are able to counteract loss processes associated with washout, whereas the warmer fall temperatures were associated with relatively slow-growing dinoflagellates that tend to experience greater washout effects (Roelke et al. 2013; Dorado et al. 2015).

During the winter, despite generally high concentrations of NO_x and NH_4^+ and near-balanced DIN:DIP ratios (15.9), phytoplankton biovolume remained low (Fig. 6). Likewise, during a winter nutrient addition bioassay in CCB, phytoplankton growth rates did not respond to added nitrogen over 48 h (Tominack 2021). Limitation of winter phytoplankton communities by low temperatures and shorter day length has been observed elsewhere (Cloern 1999; Fisher et al. 1999; Lomas and Glibert 1999; Örnólfsdóttir et al. 2004; Cira et al. 2016).

Biovolume of each of the four major taxonomic groups investigated here also varied in unimodal patterns, and the timing of peak biovolume for each group reflected known physiological tolerances and environmental condition preferences. These patterns were well represented through the creation of a conceptual diagram (Fig. 9). The winter community tended to be dominated by diatoms, with all other groups demonstrating significantly lower biovolume during winter compared to other seasons. Diatoms are known to be favored when temperatures are lower, the water column is well mixed, and concentrations of nutrients, especially NO_x, are relatively high (Cloern and Dufford 2005; Suggett et al. 2009; Baek et al. 2015). During the spring, the community was more diverse, with diatoms, picocyanobacteria, and picoeukaryotes all demonstrating higher biovolume than summer (except picocyanobacteria), fall, and winter. Wind speed was higher during the spring than other seasons and was positively correlated with diatom biovolume, which is consistent with observations that diatoms are favored in more turbulent environments (Cloern and Dufford 2005; Baek et al. 2015). The growing importance of picocyanobacteria and picoeukaryotes during the spring was likely related to their preference for warmer temperatures (Worden et al. 2004; Gaulke et al. 2010; Paerl et al. 2020) and ability to be strong competitors for nutrients under both limiting (Agawin et al. 2000) and replete conditions (Gaulke et al. 2010). The summer and fall communities were also generally diverse, though the prevalence of dinoflagellates increased while the prevalence of diatoms and picoeukaryotes declined. In the summer, increased availability of reduced N forms (Glibert et al. 2016; Shangguan et al. 2017), decreased frequency of precipitation events, increased salinity, and increased water column stability (Paerl and Justić 2013; Baek et al. 2015; Dorado et al. 2015), as well as increased temperatures (Paerl et al. 2014; Dorado et al. 2015), likely drove the shift from diatom to dinoflagellate and picocyanobacteria dominance. During the fall of 2016, there was also a short-lived *K. brevis* red tide. *K. brevis* blooms are a frequent occurrence in the CCB system and have been shown to be inversely related to El Niño conditions and positively related

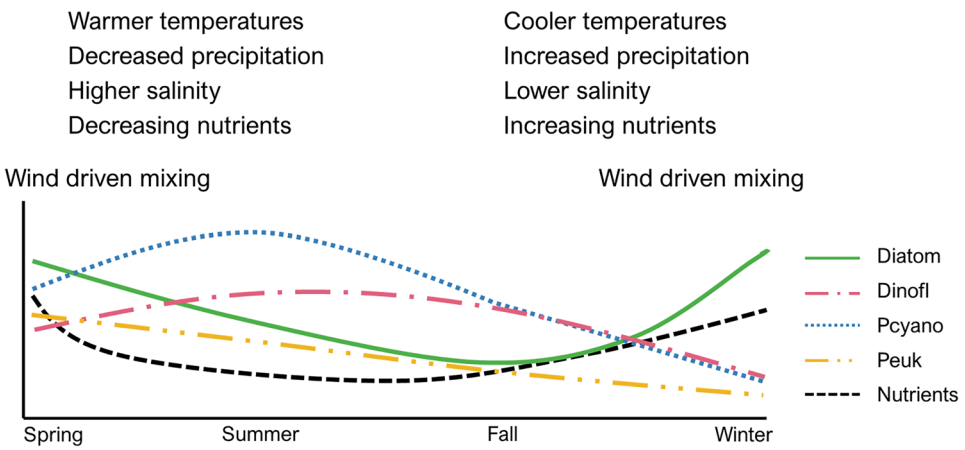

Fig. 9 Conceptual figure describing the variability in biovolume of the diatoms, dinoflagellates, picocyanobacteria, and picoeukaryotes in relation to environmental conditions. Figure 9 was created using MSOffice

to salinity (Tominack et al. 2020). During late summer-early fall of 2017, Hurricane Harvey made landfall on the south Texas coast and during 2018, El Niño conditions resulted in prolonged rainfall, which may have prevented significant *K. brevis* presence in the system during these times.

Spatially, phytoplankton biovolume reflected both nutrient conditions and proximity to freshwater inflows (Bonilla et al. 2005; Roelke et al. 2013; Dorado et al. 2015). The lowest phytoplankton biovolume was observed at Cole Park where, despite higher inputs of watershed-derived nutrients, loss processes related to hydraulic flushing were likely most pronounced. The next lowest biovolume was observed at the Laguna Madre where nutrient concentrations tended to be lower than at all other sites. At this site, there were moderate increases in phytoplankton biovolume as salinity began to increase following precipitation-driven declines (Fig. 8), supporting a role for nutrient availability in regulating phytoplankton biovolume when the effects of washout are less pronounced. Overall, the Canal site demonstrated the highest phytoplankton biovolume and occasional occurrence of very high biovolume blooms. Nutrient concentrations (especially NH_4^+) were also generally high at the Canal site. The highly restricted nature of canal systems (Maxted et al. 1997) likely contributed to the accumulation of nutrients, phytoplankton, and limited hydraulic flushing observed at this site. This finding is in line with results from other studies demonstrating generally high phytoplankton biomass in canals compared to open portions of bay systems (Maxted et al. 1997; Ma et al. 2006). Additionally, the occurrence of high biomass blooms of dinoflagellates and raphidophytes following pulsed nutrient inputs as seen here in the Canal site (Fig. 8) has also been documented in dead-end canal systems in coastal Delaware (Bourdelais et al. 2002; Ma et al. 2006). The relationship between freshwater flushing, nutrient conditions, and phytoplankton biovolume can be readily seen in the conceptual figure (Fig. 10).

Spatial variability in the prevalence of the four major taxonomic groups investigated here was not as pronounced as seasonal variability. Diatom biovolume was higher at Packery Channel compared to all other sites, with little variability found among the remaining sites (Fig. 7). Tidal exchange with the Gulf of Mexico was likely influential in the prevalence of diatoms observed at this site. Diatoms are known to be important contributors to nearshore coastal phytoplankton communities throughout the northwestern Gulf of Mexico, where rapid growth rates help to balance growth and loss processes in this highly dynamic environment (Lambert et al. 1999; Chakraborty and Lohrenz 2015; Anglés et al. 2019). Dinoflagellate biovolume tended to be higher at the Canal site than all other sites and lower at the Cole Park site than all sites other than Packery Channel. At the Canal site, the generally calm water conditions coupled with high concentrations of reduced N forms likely supported the higher biovolume of dinoflagellates observed here, whereas the high rates of hydraulic flushing at Cole Park and constant water movement via tidal exchange at Packery Channel were unfavorable for the accumulation of relatively slow-growing dinoflagellates (Glibert et al. 2016; Shangguan et al. 2017;

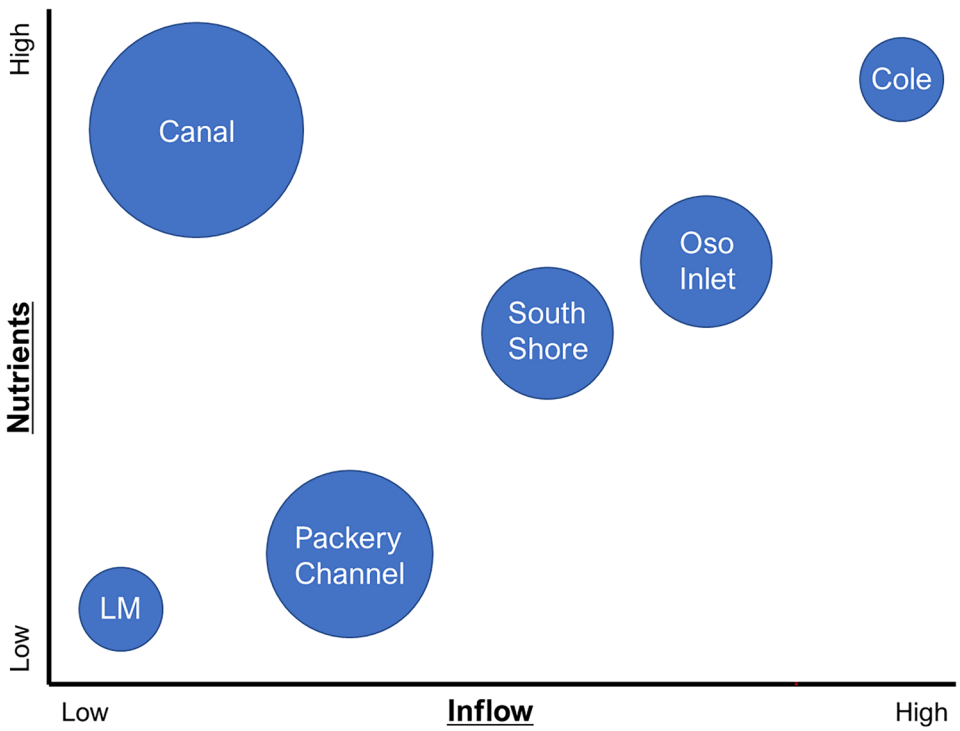

Fig. 10 Conceptual figure demonstrating the interrelatedness of freshwater inflows and nutrients in driving phytoplankton biovolume. Figure 10 was created using MSOffice

Paerl and Justić 2013; Baek et al. 2015; Dorado et al. 2015). This is further supported by the positive correlation between salinity and dinoflagellates observed here (Table 6). Picocyanobacteria and picoeukaryotes both tended to be more prevalent at the Canal and Oso Inlet sites compared to others. Picocyanobacteria and picoeukaryotes are both known to be favored by reduced N forms (Glibert et al. 2010, 2016; Shangguan et al. 2017), though both groups have also been shown to respond to pulsed inputs of oxidized N (Agawin et al. 2000; Tominack 2021). At Oso Inlet, despite closer proximity to freshwater inflows from Oso Creek, export of picocyanobacteria and picoeukaryotes from upper reaches of Oso Bay may have contributed to the high prevalence of these groups, as has been seen in other systems (Reyna et al. 2017; Paerl et al. 2020). At the Canal site, the generally calm conditions and limited flushing during precipitation events may have allowed both picocyanobacteria and picoeukaryotes to flourish (Gaulke et al. 2010; Zhang et al. 2013; Dorado et al. 2015; Paerl et al. 2020).

Future Implications

Phytoplankton biovolume in the CCB system was related to the availability of nutrients, but factors such as freshwater inflows, precipitation, hydrological modifications, and temperature were also important in driving whole community and major taxonomic group dynamics. These findings are similar to those from other low-inflow estuaries from around the globe (Gilabert 2001; Hemraj et al. 2017; Reyna et al. 2017; Cira et al. 2021; Glibert et al. 2021; Lemley et al. 2017, 2021). The generally low riverine inflows and the limited spatial extent of influence from sources such as stormwater runoff and wastewater may, however, act to buffer the CCB system from displaying symptoms of eutrophication in the present, at least compared to increased susceptibility of other low-inflow estuaries (Wetz et al. 2017; Lemley et al. 2017, 2021). Due to the shore-based nature of the sites employed during this study, it was difficult to explore the spatial extent of the effects of precipitation-driven freshwater inflows. A study by Chin et al. (in press) helps to elucidate this in the context of the central portion of CCB. The El Niño–driven precipitation during the summer-fall of 2018 elicited a suppression of phytoplankton biovolume in the upper reaches of Nueces Bay but was related to increased phytoplankton biovolume in the central portion of CCB (ship channel). Additionally, only relatively modest increases in phytoplankton biovolume near Mustang Island in the southern reaches of CCB were observed during this period. These results indicate that even under abnormally high precipitation and inflow conditions, there is relatively little connectivity between areas of CCB receiving freshwater inflows and areas of CCB that do not directly receive freshwater inflows. The limited influence of precipitation-driven inflow events at the South Shore site (~90 m from stormwater drain) compared to the Cole Park site (at a stormwater drain) seen in the environmental data (Fig. 3) and in phytoplankton biovolume (Fig. 6) also supports the conclusion that the spatial extent of freshwater inflows is limited in the CCB system.

Under future climate change scenarios, the Texas Coastal Bend region is predicted to become warmer and drier overall, with continued population growth and expanding urban areas (Pachauri et al. 2014; Nielsen-Gammon et al. 2020; U.S. Census Bureau). There is potential for these changes to affect the estuarine environment in general, and primary producers specifically. As the region becomes drier and freshwater withdrawals to meet human demands increase, further decreases in freshwater inflows are expected to result in decreases in riverine nutrient inputs and increased salinity/residence time throughout the system. The increased prevalence of dinoflagellates and picocyanobacteria during periods of low precipitation and increased concentrations of reduced N forms (summer-early fall), combined with the increased prevalence observed at the Canal site, indicate that these groups may become more persistently dominant in the future (Ferreira et al. 2005; Glibert et al. 2005; Altman and Paerl 2012; de Souza et al. 2014). Documented linkages between the frequency of *K. brevis* red tides and salinity also indicate that conditions could become more favorable for the success of transported blooms under future scenarios (Tominack et al. 2020). It can also be expected that localized phytoplankton blooms will continue to occur and possibly expand if there is an expansion of man-made canals in this region. Furthermore, increased winter-spring temperatures will likely shift the spring bloom forward in time (Guinder et al. 2010; Winder and Sommer 2012; Nohe et al. 2020), potentially resulting in earlier depletion of NO_x and succession from diatoms to picophytoplankton and dinoflagellates, which will have important implications for system productivity and food webs. Further work investigating the response of phytoplankton to a range of freshwater inflow conditions, nutrients, and temperature increases at different times of year is needed to better resolve future impacts and changes. Likewise, freshwater inflow management assessments often do not explicitly take phytoplankton community composition or HAB formation potential into account. In a system such as CCB where decreased flows have the potential to lead to shifts in total phytoplankton biovolume and community composition, as well as the occurrence of *K. brevis* red tides (see Tominack et al. 2020), assessing the role freshwater management may play in phytoplankton dynamics will be paramount.

Supplementary Information The online version contains supplementary material available at https://doi.org/10.1007/s12237-022-01137-y.

Declarations

Competing Interests The authors declare no competing interests.

References

Agawin, N.S.R., C.M. Duarte, and S. Agustí. 2000. Nutrient and temperature control of the contribution of picoplankton to phytoplankton biomass and production. *Limnology and Oceanography* 45: 591–600. https://doi.org/10.4319/lo.2000.45.3.0591.

Altman, J.C., and H.W. Paerl. 2012. Composition of inorganic and organic nutrient sources influences phytoplankton community structure in the New River Estuary, North Carolina. *Aquatic Ecology* 46 (3): 269–282. https://doi.org/10.1007/s10452-012-9398-8.

Anglés, S., A. Jordi, D.W. Henrichs, and L. Campbell. 2019. Influence of coastal upwelling and river discharge on the phytoplankton community composition in the northwestern Gulf of Mexico. *Progress in Oceanography* 173: 26–36. https://doi.org/10.1016/j.pocean.2019.02.001.

Baek, S.H., D. Kim, M. Son, S.M. Yun, and Y.O. Kim. 2015. Seasonal distribution of phytoplankton assemblages and nutrient-enriched bioassays as indicators of nutrient limitation of phytoplankton growth in Gwangyang Bay, Korea. *Estuarine, Coastal and Shelf Science* 163: 265–278. https://doi.org/10.1016/j.ecss.2014.12.035.

Bonilla, S., D. Conde, L. Aubriot, and M.D.C. Pérez. 2005. Influence of hydrology on phytoplankton species composition and life strategies in a subtropical coastal lagoon periodically connected with the Atlantic Ocean. *Estuaries* 28: 884–895. https://doi.org/10.1007/BF02696017.

Borcard, D.P., P. Legendre, and F. Gillet. 2011. *Numerical Ecology with R*. New York, NY: Springer Publishing.

Bourdelais, A.J., C.R. Tomas, J. Naar, J. Kubanek, and D.G. Baden. 2002. New fish-killing alga in coastal Delaware produces neurotoxins. *Environmental Health Perspectives* 110: 465–470.

Bricker, S.B., B. Longstaff, W. Dennison, A. Jones, K. Boicourt, C. Wicks, and J. Woerner. 2008. Effects of nutrient enrichment in the nation's estuaries: A decade of change. *Harmful Algae* 8: 21–32. https://doi.org/10.1016/j.hal.2008.08.028.

Bruesewitz, D.A., W.S. Gardner, R.F. Mooney, and E.J. Buskey. 2015. Seasonal water column NH4+ cycling along a semi-arid subtropical river-estuary continuum: Responses to episodic events and drought conditions. *Ecosystems* 18: 792–812. https://doi.org/10.1007/s10021-015-9863-z.

Bugica, K., B. Sterba-Boatwright, and M.S. Wetz. 2020. Water quality trends in Texas estuaries. *Marine Pollution Bulletin* 152: 110903. https://doi.org/10.1016/j.marpolbul.2020.110903.

Burkholder, J.A.M., P.M. Glibert, and H.M. Skelton. 2008. Mixotrophy, a major mode of nutrition for harmful algal species in eutrophic waters. *Harmful Algae* 8: 77–93. https://doi.org/10.1016/j.hal.2008.08.010.

Caffrey, J.M., T.P. Chapin, H.W. Jannasch, and J.C. Haskins. 2007. High nutrient pulses, tidal mixing and biological response in a small California estuary: Variability in nutrient Concentrations from decadal to hourly time scales. *Estuarine, Coastal and Shelf Science* 71: 368–380. https://doi.org/10.1016/j.ecss.2006.08.015.

Chakraborty, S., and S.E. Lohrenz. 2015. Phytoplankton community structure in the river-influenced continental margin of the northern Gulf of Mexico. *Marine Ecology Progress Series* 521: 31–47. https://doi.org/10.3354/meps11107.

Chin, T.L. 2020. *Comparison of phytoplankton biomass and community composition in three Texas estuaries differing in freshwater inflow regime*. Texas A&M University – Corpus Christi Master's Thesis.

Cira, E.K., H.W. Paerl, and M.S. Wetz. 2016. Effects of nitrogen availability and form on phytoplankton growth in a eutrophied estuary (Neuse River Estuary, NC, USA). *PLoS ONE* 11: e0160663. https://doi.org/10.1371/journal.pone.0160663.

Cira, E.K., T.A. Palmer, and M.S. Wetz. 2021. Phytoplankton dynamics in a low-inflow estuary (Baffin Bay, TX) during drought and high-rainfall conditions associated with an El Niño event. *Estuaries and Coasts*. https://doi.org/10.1007/s12237-021-00904-7.

Clarke, K.R., and R.N. Gorley. 2015. *Getting started with PRIMER v7*. PRIMER-E: Plymouth, Plymouth Marine Laboratory.

Cloern, J.E. 1999. The relative importance of light and nutrient limitation of phytoplankton growth: A simple index of coastal ecosystem sensitivity to nutrient enrichment. *Aquatic Ecology* 33: 3–19.

Cloern, J.E. 2019. Patterns, pace, and processes of water-quality variability in a long-studied estuary. *Limnology and Oceanography* 64: S192–S208. https://doi.org/10.1002/lno.10958.

Cloern, J.E., and A.D. Jassby. 2008. Complex seasonal patterns of primary producers at the land-sea interface. *Ecology Letters* 11: 1294–1303. https://doi.org/10.1111/j.1461-0248.2008.01244.x.

Cloern, J.E., and A.D. Jassby. 2010. Patterns and scales of phytoplankton variability in estuarine-coastal ecosystems. *Estuaries and Coasts* 33: 230–241. https://doi.org/10.1007/s12237-009-9195-3.

Cloern, J.E., and R. Dufford. 2005. Phytoplankton community ecology: Principles applied in San Francisco Bay. *Marine Ecology Progress Series* 285: 11–28. https://doi.org/10.3354/meps285011.

Cloern, J.E., S.Q. Foster, and A.E. Kleckner. 2014. Phytoplankton primary production in the world's estuarine-coastal systems. *Biogeosciences* 11: 2477–2501. https://doi.org/10.5194/bg-11-2477-2014.

Davidson, K., R.J. Gowen, P.J. Harrison, L.E. Fleming, P. Hoagland, and G. Moschonas. 2014. Anthropogenic nutrients and harmful algae in coastal waters. *Journal of Environmental Management* 146: 206–216. https://doi.org/10.1016/j.jenvman.2014.07.002.

de Souza, K.B., T. Jephson, T.B. Hasper, and P. Carlsson. 2014. Species-specific dinoflagellate vertical distribution in temperature-stratified waters. *Marine Biology* 161: 1725–1734. https://doi.org/10.1007/s00227-014-2446-2.

Dillon, K.S., and J.P. Chanton. 2005. Nutrient transformations between rainfall and stormwater runoff in an urbanized coastal environment: Sarasota Bay, Florida. *Limnology and Oceanography* 50: 62–69. https://doi.org/10.4319/lo.2005.50.1.0062.

Dorado, S., T. Booe, J. Steichen, A.S. McInnes, R. Windham, A. Shepard, A.E.B. Lucchese, et al. 2015. Towards an understanding of the interactions between freshwater inflows and phytoplankton communities in a subtropical estuary in the Gulf of Mexico. *PLoS ONE* 10: e0130931. https://doi.org/10.1371/journal.pone.0130931.

Douglas, A.R., D. Murgulet, and P.A. Montagna. 2021. Hydroclimatic variability drives submarine groundwater discharge and nutrient fluxes in an anthropogenically disturbed, semi-arid estuary. *Science of the Total Environment* 755: 142574. https://doi.org/10.1016/j.scitotenv.2020.142574.

Dunn, D.E. 1996. *Trends in nutrient inflows to the Gulf of Mexico from streams draining the conterminous United States, 1972–93*. U.S. Geological Survey Water-Resources Investigations Report 96–4113: 68.

Ferreira, J.G., W.J. Wolff, T.C. Simas, and S.B. Bricker. 2005. Does biodiversity of estuarine phytoplankton depend on hydrology? *Ecological Modelling* 187: 513–523. https://doi.org/10.1016/j.ecolmodel.2005.03.013.

Fisher, T.R., A.B. Gustafson, K. Sellner, R. Lacouture, L.W. Haas, R.L. Wetzel, R. Magnien, D. Everitt, B. Michaels, and R. Karrh. 1999. Spatial and temporal variation of resource limitation in Chesapeake Bay. *Marine Biology* 133: 763–778. https://doi.org/10.1007/s002270050518.

Flint, R. W. 1984. Phytoplankton production in the Corpus Christi Bay estuary. *Contributions in Marine Science* 27: 65–83.

Gaulke, A.K., M.S. Wetz, and H.W. Paerl. 2010. Picophytoplankton: A major contributor to planktonic biomass and primary production in a eutrophic, river-dominated estuary. *Estuarine, Coastal and Shelf Science* 90: 45–54. https://doi.org/10.1016/j.ecss.2010.08.006.

Geyer, N.L., M. Huettel, and M.S. Wetz. 2018. Phytoplankton spatial variability in the river-dominated estuary, Apalachicola Bay, Florida. *Estuaries and Coasts* 41: 2024–2038. https://doi.org/10.1007/s12237-018-0402-y.

Gilabert, J. 2001. Seasonal plankton dynamics in a Mediterranean hypersaline coastal lagoon: The Mar Menor. *Journal of Plankton Research* 23: 207–217.

Glibert, P.M., and J.A.M. Burkholder. 2011. Harmful algal blooms and eutrophication: "strategies" for nutrient uptake and growth outside the Redfield comfort zone. *Chinese Journal of Oceanology and Limnology* 29: 724–738. https://doi.org/10.1007/s00343-011-0502-z.

Glibert, P.M., C.A. Heil, C.J. Madden, and S.P. Kelly. 2021. Dissolved organic nutrients at the interface of fresh and marine waters: flow regime changes, biogeochemical cascades and picocyanobacterial blooms – the example of Florida Bay, USA. *Biogeochemistry*. https://doi.org/10.1007/s10533-021-00760-4.

Glibert, P.M., D.M. Anderson, P. Gentien, E. Granéli, and K.G. Sellner. 2005. The global, complex phenomena of harmful algal blooms. *Oceanography* 18: 136–147. https://doi.org/10.1016/B978-0-12-385876-4.00020-7.

Glibert, P.M., F.P. Wilkerson, R.C. Dugdale, J.A. Raven, C.L. Dupont, P.R. Leavitt, A.E. Parker, J.M. Burkholder, and T.M. Kana. 2016. Pluses and minuses of ammonium and nitrate uptake and assimilation by phytoplankton and implications for productivity and community composition, with emphasis on nitrogen-enriched conditions. *Limnology and Oceanography* 61: 165–197. https://doi.org/10.1002/LNO.10203@10.1002/(ISSN)1939-5590.STABLE-ISOTOPES.

Glibert, P.M., J.N. Boyer, C.A. Heil, C.J. Madden, B. Sturgis, and C.S. Wazniak. 2010. Blooms in lagoons: Different from those of river-dominated estuaries. In *Coastal Lagoons: Critical Habitats of Environmental Change*, ed. M.J. Kennish and H.W. Paerl, 91–113. Boca Raton: CRC Press.

Guinder, V.A., C.A. Popovich, J.C. Molinero, and G.M.E. Perillo. 2010. Long-term changes in phytoplankton phenology and community structure in the Bahía Blanca Estuary, Argentina. *Marine Biology* 157: 2703–2716. https://doi.org/10.1007/s00227-010-1530-5.

Hemraj, D.A., M.A. Hossain, Q. Ye, J.G. Qin, and S.C. Leterme. 2017. Plankton bioindicators of environmental conditions in coastal lagoons. *Estuarine, Coastal and Shelf Science* 184: 102–114.

Holland, J.S., N.J. Maciolek, R.D. Kalke, L. Mullins, and C.H. Oppenheimer. 1975. A benthos and plankton study of the Corpus Christi, Copano and Aransas bay systems III. Report on Data Collected During the Period July 1974-May 1975 and Summary of the Three-year Project. Texas Water Development Board.

Hothorn, T., F. Bretz, and P. Westfall. 2008. Simultaneous inference in general parametric models. *Biometrical Journal* 50: 346–363.

Islam, M.S., J.S. Bonner, B.L. Edge, and C.A. Page. 2014. Hydrodynamic characterization of Corpus Christi Bay through modeling and observation. *Environmental Monitoring and Assessment* 186: 7863–7876. https://doi.org/10.1007/s10661-014-3973-5.

Jordan, T.E., D.E. Weller, and C.E. Pelc. 2018. Effects of local watershed land use on water quality in Mid-Atlantic coastal bays and subestuaries of the Chesapeake Bay. *Estuaries and Coasts* 41: 38–53. https://doi.org/10.1007/s12237-017-0303-5.

Lambert, C.D., T.S. Bianchia, and P.H. Santschi. 1999. Cross-shelf changes in phytoplankton community composition in the Gulf of Mexico (Texas shelf/slope): The use of plant pigments as biomarkers. *Continental Shelf Research* 19: 1–21. https://doi.org/10.1016/S0278-4343(98)00075-2.

Largier, J.L., and D.M. Behrens. 2010. *Hydrography of the Russian River Estuary summer-fall 2009*. Suffolk County Water Authority Submitted report.

Lemley, D.A., J.B. Adams, and S. Taljaard. 2017. Comparative assessment of two agriculturally-influenced estuaries: Similar pressure, different response. *Marine Pollution Bulletin* 117: 136–147.

Lemley, D.A., S.J. Lamberth, W. Manuel, M. Nunes, G.M. Rishworth, L. van Niekerk, and J.B. Adams. 2021. Effective management of closed hypereutrophic estuaries requires catchment-scale interventions. *Frontiers in Marine Science*. https://doi.org/10.3389/fmars.2021.688933.

Lomas, M.W., and P.M. Glibert. 1999. Interactions between NH4+ and NO3- uptake and assimilation: Comparisons of diatoms and dinoflagellates at several growth temperatures. *Marine Biology* 133: 541–551. https://doi.org/10.1007/s002270050494.

Ma, S., E.B. Whereat, and G.W. Luther III. 2006. Shift of algal community structure in dead end lagoons of the Delaware Inland Bays during seasonal anoxia. *Aquatic Microbial Ecology* 44: 279–290.

Mallin, M.A., V.L. Johnson, and S.H. Ensign. 2009. Comparative impacts of stormwater runoff on water quality of an urban, a suburban, and a rural stream. *Environmental Monitoring and Assessment* 159: 475–491. https://doi.org/10.1007/s10661-008-0644-4.

Mallin, M.A., H.W. Paerl, J. Rudek, and P.W. Bates. 1993. Regulation of estuarine primary production by watershed rainfall and river flow. *Marine Ecology Progress Series* 93: 199–203.

Maxted, J.R., S.B. Weisberg, J.C. Chaillou, R.A. Eskin, and F.W. Kutz. 1997. The ecological condition of dead-end canals of the Delaware and Maryland coastal bays. *Estuaries* 20: 319–327. https://doi.org/10.2307/1352347.

McCarthy, M.D., and D.A. Bronk. 2008. Analytical methods for the study of nitrogen. In *Nitrogen in the Marine Environment*, 1219–1275. Elsevier Inc. https://doi.org/10.1016/B978-0-12-372522-6.00028-1.

Montagna, P.A., E.M. Hill, and B. Moulton. 2009. Role of science-based and adaptive management in allocating environmental flows to the Nueces Estuary, Texas, USA. *WIT Transactions on Ecology and the Environment* 122: 559–570. https://doi.org/10.2495/ECO090511.

Morin, J., and J.W. Morse. 1999. Ammonium release from resuspended sediments in the Laguna Madre estuary. *Marine Chemistry* 65: 97–110. https://doi.org/10.1016/S0304-4203(99)00013-4.

Nielsen-Gammon, J., J. Banner, B. Cook, D. Tremaine, C. Wong, R. Mace, H. Gao, et al. 2020. Unprecedented drought challenges for Texas water resources in a changing climate: what do researchers and stakeholders need to know? *Earth's Future* 8: e2020EF001552. https://doi.org/10.1029/2020EF001552.

Nohe, A., A. Goffin, L. Tyberghein, R. Lagring, K. de Cauwer, W. Vyverman, and K. Sabbe. 2020. Marked changes in diatom and dinoflagellate biomass, composition and seasonality in the Belgian Part of the North Sea between the 1970s and 2000s. *Science of the Total Environment* 716: 136316. https://doi.org/10.1016/j.scitotenv.2019.136316.

Örnólfsdóttir, E.B., S.E. Lumsden, and J.L. Pinckney. 2004. Nutrient pulsing as a regulator of phytoplankton abundance and community composition in Galveston Bay, Texas. *Journal of Experimental Marine Biology and Ecology* 303: 197–220. https://doi.org/10.1016/j.jembe.2003.11.016.

Pachauri, R.K., M.R. Allen, V.R. Barros, J. Broome, W. Cramer, R. Christ, J.A. Church, et al. 2014. *Climate Change 2014: Synthesis Report. Contribution of Working Groups I, II and III to the Fifth Assessment Report of the Intergovernmental Panel on Climate Change*. IPCC R. K. Pachauri & L. Meyer, Eds.

Paerl, H.W., and D. Justić. 2013. Estuarine phytoplankton. In *Estuarine ecology*, 2nd ed., 85–110. Wiley Online Library.

Paerl, H.W., K.L. Rossignol, S.N. Hall, B.L. Peierls, and M.S. Wetz. 2010. Phytoplankton community indicators of short- and long-term ecological change in the anthropogenically and climatically impacted neuse river estuary, North Carolina, USA. *Estuaries and Coasts* 33: 485–497. https://doi.org/10.1007/s12237-009-9137-0.

Paerl, H.W., N.S. Hall, B.L. Peierls, and K.L. Rossignol. 2014. Evolving paradigms and challenges in estuarine and coastal eutrophication dynamics in a culturally and climatically stressed world. *Estuaries and Coasts* 37: 243–258. https://doi.org/10.1007/s12237-014-9773-x.

Paerl, R.W., R.E. Venezia, J.J. Sanchez, and H.W. Paerl. 2020. Picophytoplankton dynamics in a large temperature estuary and impacts of extreme storm events. *Scientific Reports* 10: 22026. https://doi.org/10.1038/s41598-020-79157-6.

Parsons, M.L., and Q. Dortch. 2002. Sedimentological evidence of an increase in Pseudo-nitzschia (Bacillariophyceae) abundance in response to coastal eutrophication. *Limnology and Oceanography* 47: 551–558. https://doi.org/10.4319/lo.2002.47.2.0551.

Paudel, B., P.A. Montagna, and L. Adams. 2015. Variations in the release of silicate and orthophosphate along a salinity gradient: Do sediment composition and physical forcing have roles? *Estuarine, Coastal and Shelf Science* 157: 42–50. https://doi.org/10.1016/j.ecss.2015.02.011.

Peierls, B.L., N.S. Hall, and H.W. Paerl. 2012. Non-monotonic responses of phytoplankton biomass accumulation to hydrologic variability: A comparison of two coastal plain north carolina estuaries. *Estuaries and Coasts* 35: 1376–1392. https://doi.org/10.1007/s12237-012-9547-2.

Pennock, J.R., J.N. Boyer, J.A. Herrera-Silveira, R.L. Iverson, T.E. Whitledge, B. Mortazavi, and F.A. Comin. 1999. Nutrient behavior and phytoplankton production in Gulf of Mexico estuaries. In *Biogeochemistry of Gulf of Mexico Estuaries*, ed. T.S. Bianchi, J.R. Pennock, and R.R. Twilley, 109–162. John Wiley and Sons Inc.

Phlips, E.J., S. Badylak, M. Christman, J. Wolny, J. Brame, J. Garland, L. Hall, et al. 2011. Scales of temporal and spatial variability in the distribution of harmful algae species in the Indian River Lagoon, Florida, USA. *Harmful Algae* 10: 277–290. https://doi.org/10.1016/j.hal.2010.11.001.

Pinckney, J.L., H.W. Paerl, M.B. Harrington, and K.E. Howe. 1998. Annual cycles of phytoplankton community-structure and bloom dynamics in the Neuse River Estuary, North Carolina. *Marine Biology* 131: 371–381. https://doi.org/10.1007/s002270050330.

Pinckney, J.L., H.W. Paerl, P. Tester, and T.L. Richardson. 2001. The role of nutrient loading and eutrophication in estuarine ecology. *Environmental Health Perspectives* 109: 699–706. https://doi.org/10.1289/ehp.01109s5699.

Pinheiro, J., D. Bates, and R Core Team. 2022. *{nlme}: Linear and Nonlinear Mixed Effects Models*. R package version 3.1-157. https://CRAN.R-project.org/package=nlme

Quigg, A., M. Al-Ansi, N.N. al Din, C.L. Wei, C.C. Nunnally, I.S. Al-Ansari, G.T. Rowe, et al. 2013. Phytoplankton along the coastal shelf of an oligotrophic hypersaline environment in a semi-enclosed marginal sea: Qatar (Arabian Gulf). *Continental Shelf Research* 60: 1–16. https://doi.org/10.1016/j.csr.2013.04.015.

Quinn, G.P., and M.J. Keough. 2002. *Experimental design and data analysis for biologists*. Cambridge University Press.

R Core Team. 2019. *R: A language and environment for statistical computing*. Vienna: Austria.

Reyna, N.E., A.K. Hardison, and Z. Liu. 2017. Influence of major storm events on the quantity and composition of particulate organic matter and the phytoplankton composition in a subtropical estuary, Texas. *Frontiers in Marine Science* 4: 43. https://doi.org/10.3389/mars.2017.00043.

Ritter, C., and P.A. Montagna. 1999. Seasonal hypoxia and models of benthic response in a Texas Bay. *Estuaries* 22: 7–20. https://doi.org/10.2307/1352922.

Roelke, D.L., H.P. Li, N.J. Hayden, C.J. Miller, S.E. Davis, A. Quigg, and Y. Buyukates. 2013. Co-occurring and opposing freshwater inflow effects on phytoplankton biomass, productivity and community composition of Galveston Bay, USA. *Marine Ecology Progress Series* 477: 61–76. https://doi.org/10.3354/meps10182.

Roelke, D.L., L.A. Cifuentes, and P.M. Eldridge. 1997. Nutrient and phytoplankton dynamics in a sewage-impacted gulf coast estuary: A field test of the PEG-model and Equilibrium Resource Competition theory. *Estuaries* 20: 725–742. https://doi.org/10.2307/1352247.

Shangguan, Y., P.M. Glibert, J.A. Alexander, C.J. Madden, and S. Murasko. 2017. Nutrients and phytoplankton in semienclosed lagoon systems in Florida Bay and their responses to changes in flow from Everglades restoration. *Limnology and Oceanography* 62: S327–S347. https://doi.org/10.1002/lno.10599.

Suggett, D.J., C.M. Moore, A.E. Hickman, and R.J. Geider. 2009. Interpretation of fast repetition rate (FRR) fluorescence: Signatures of phytoplankton community structure versus physiological state. *Marine Ecology Progress Series* 376: 1–19. https://doi.org/10.3354/meps07830.

Sun, J., and D. Liu. 2003. Geometric models for calculating cell biovolume and surface area for phytoplankton. *Journal of Plankton Research* 25: 1331–1346. https://doi.org/10.1093/plankt/fbg096.

Sverdrup, H.U. 1953. On conditions for the vernal blooms of phytoplankton. *Journal Du Conseil* 18: 287–295.

Tominack, S.A. 2021. *Phytoplankton dynamics in an urbanizing South Texas estuary, Corpus Christi Bay, Texas*. Texas A&M University – Corpus Christi Doctoral Dissertation.

Tominack, S.A., K.Z. Coffey, D. Yoskowitz, G. Sutton, and M.S. Wetz. 2020. An assessment of trend in the frequency and duration of *Karenia brevis* red tide blooms on the South Texas coast (western Gulf of Mexico). *PLoS ONE* 15: e0239309. https://doi.org/10.1371/journal.pone.0239309.

Turner, E.L., B. Paudel, and P.A. Montagna. 2015. Baseline nutrient dynamics in shallow well mixed coastal lagoon with seasonal harmful algal blooms and hypoxia formation. *Marine Pollution Bulletin* 96: 456–462. https://doi.org/10.1016/j.marpolbul.2015.05.005.

Wang, H., X. Hu, M.S. Wetz, and K.C. Hayes. 2018. Oxygen consumption and organic matter remineralization in two subtropical, eutrophic embayments. *Environmental Science and Technology* 52: 13004–13014. https://doi.org/10.1021/acs.est.8b02971.

Ward, G.H. 1997. Processes and trends of circulation within the Corpus Christi National Estuary Program study area. Report to Coastal Bend Bays and Estuaries Program. Publication No CBBNEP-21.

Wetz, M.S., E.K. Cira, B. Sterba-Boatwright, P.A. Montagna, T.A. Palmer, and K.C. Hayes. 2017. Exceptionally high organic nitrogen concentrations in a semi-arid South Texas estuary susceptible to brown tide blooms. *Estuarine, Coastal and Shelf Science* 188: 27–37. https://doi.org/10.1016/j.ecss.2017.02.001.

Wetz, M.S., K.C. Hayes, K.V.B. Fisher, L. Price, and B. Sterba-Boatwright. 2016. Water quality dynamics in an urbanizing subtropical estuary (Oso Bay, Texas). *Marine Pollution Bulletin* 104: 44–53. https://doi.org/10.1016/j.marpolbul.2016.02.013.

Wetz, M.S., E.A. Hutchinson, R.S. Lunetta, H.W. Paerl, and J.C. Taylor. 2011. Severe droughts reduce estuarine primary productivity with cascading effects on higher trophic levels. *Limnology and Oceanography* 56: 627–638.

Winder, M., and U. Sommer. 2012. Phytoplankton response to a changing climate. *Hydrobiologia* 698: 5–16. https://doi.org/10.1007/s10750-012-1149-2.

Worden, A.Z., J.K. Nolan, and B. Palenik. 2004. Assessing the dynamics and ecology of marine picophytoplankton: The importance of the eukaryotic component. *Limnology and Oceanography* 49: 168–179. https://doi.org/10.4319/lo.2004.49.1.0168.

Yang, Y.Y., and G.S. Toor. 2017. Sources and mechanisms of nitrate and orthophosphate transport in urban stormwater runoff from

residential catchments. *Water Research* 112: 176–184. https://doi.org/10.1016/j.watres.2017.01.039.

Yeager, K.M., P.H. Santschi, K.J. Schindler, M.J. Andres, and E.A. Weaver. 2006. The relative importance of terrestrial versus marine sediment sources to the Nueces-Corpus Christi Estuary, Texas: An isotopic approach. *Estuaries and Coasts* 29: 443–454. https://doi.org/10.1007/BF02784992.

Zhang, X., Z. Shi, Q. Liu, F. Ye, L. Tian, and X. Huang. 2013. Spatial and temporal variations of picoplankton in three contrasting periods in the Peral River Estuary, South China. *Continental Shelf Research* 56: 1–12. https://doi.org/10.1016/j.csr.2013.01.015.

Zingone, A., E.J. Phlips, and P.J. Harrison. 2010. Multiscale variability of twenty-two coastal phytoplankton time series: A global scale comparison. *Estuaries and Coasts* 33: 224–229. https://doi.org/10.1007/s12237-009-9261-x.